AN ARTIFICIAL NEURAL NETWORK TOOL TO ESTIMATE WAVE OVERTOPPING AT VERTICAL WALLS WITH STILLING WAVE BASIN STRUCTURES

A THESIS SUBMITTED TO
THE GRADUATE SCHOOL OF NATURAL AND APPLIED SCIENCES
OF
MIDDLE EAST TECHNICAL UNIVERSITY

BY

UTKU UZUN

IN PARTIAL FULFILLMENT OF THE REQUIREMENTS
FOR
THE DEGREE OF MASTER OF SCIENCE
IN
CIVIL ENGINEERING

DECEMBER 2023

Approval of the thesis:

AN ARTIFICIAL NEURAL NETWORK TOOL TO ESTIMATE WAVE OVERTOPPING AT VERTICAL WALLS WITH STILLING WAVE BASIN STRUCTURES

submitted by **UTKU UZUN** in partial fulfillment of the requirements for the degree of **Master of Science** i**n Civil Engineering, Middle East Technical University** by,

Prof. Dr. Halil Kalıpçılar
Dean, Graduate School of **Natural and Applied Sciences** _____

Prof. Dr. Erdem Canbay
Head of the Department, **Civil Engineering** _____

Assist. Prof. Dr. Gülizar Özyurt Tarakcıoğlu
Supervisor, **Civil Engineering, METU** _____

Assist. Prof. Dr. Doğan Kısacık
Co-Supervisor, **Civil Engineering, Izmir Institute of Technology** _____

Examining Committee Members:

Assoc. Prof. Dr. Elif Oğuz
Civil Engineering, METU _____

Assist. Prof. Dr. Gülizar Özyurt Tarakcıoğlu
Civil Engineering, METU _____

Assist. Prof. Dr. Cüneyt Baykal
Civil Engineering, METU _____

Prof. Dr. Kubilay Cihan
Civil Engineering, Kırıkkale University _____

Assist. Prof. Dr. Doğan Kısacık
Civil Engineering, Izmir Institute of Technology _____

Date: 06.12.2023

I hereby declare that all information in this document has been obtained and presented in accordance with academic rules and ethical conduct. I also declare that, as required by these rules and conduct, I have fully cited and referenced all material and results that are not original to this work.

Name Last name : Utku Uzun

Signature :

ABSTRACT

AN ARTIFICIAL NEURAL NETWORK TOOL TO ESTIMATE WAVE OVERTOPPING AT VERTICAL WALLS WITH STILLING WAVE BASIN STRUCTURES

Uzun, Utku
Master of Science, Civil Engineering
Supervisor: Assist. Prof. Dr Gülizar Özyurt Tarakcıoğlu
Co-Supervisor: Assist. Prof. Dr. Doğan Kısacık

December 2023, 85 pages

Estimating wave overtopping values in coastal defense structures is a very important phenomenon in coastal engineering. Due to the complex behavior of waves, most of the existing wave overtopping estimation methods are empirical and valid for limited conditions. As a new design approach, artificial neural network (ANN) tools are started to be developed. The available ANN tools such as The Overtopping-Neural Network tool can calculate overtopping values at sloped rubble mound structures, and simple vertical walls. However, it cannot calculate wave overtopping values at vertical walls that have bullnose, promenade, and stilling wave basins (SWB). SWB, in shorelines where social and recreational facilities are done regularly, can be an efficient way of designing sea defense structures, since it can result in lower wave overtopping results in shorelines with lower crest level values.

In this study, an ANN tool that calculates overtopping discharges at vertical seawalls with SWB is developed. A database for training and testing of the ANN is collected. The most efficient architecture was analyzed and selected with Grid Search method. The new ANN tool is evaluated against wave overtopping discharge empirical

formulas in the literature and The Overtopping-Neural Network tool adopted by EurOtop (2018).

The new ANN tool shows very good performance with high accuracy metrics on both plain vertical walls and vertical walls with SWB. The new ANN performed better than The Overtopping-Neural Network on plain vertical walls. In addition, the new ANN tool performed better than empirical formulas on plain vertical walls and as well as empirical formulas on vertical walls with SWB.

Keywords: Wave Overtopping, Machine Learning, Artificial Neural Networks, Stilling Wave Basin

ÖZ

DURGUN DALGA HAVUZU İLE BÜTÜNLEŞİK KIYI DUVARLARINDAKİ DALGA AŞMASINI TAHMİN EDEN YAPAY SİNİR AĞLARI ARACI ÇALIŞMASI

Uzun, Utku
Yüksek Lisans, İnşaat Mühendisliği
Tez Yöneticisi: Dr. Öğr. Üy. Gülizar Özyurt Tarakcıoğlu
Ortak Tez Yöneticisi: Dr. Öğr. Üy. Doğan Kısacık

Aralık 2023, 85 sayfa

Kıyı koruma yapılarında, dalga aşması tahmini çok önemli bir konudur. Dalgaların kompleks yapılarından dolayı, dalga aşması tahmini için kullanılan yöntemlerin çoğu empirik veya limitli yöntemlerden oluşmaktadır. Yeni bir tasarım yöntemi olarak yapay sinir ağları (YSA) kullanılmaya başlanmıştır. Literaturde bulunan The Overtopping-Neural Network aracı farklı dalga koşulları ve kıyı savunması yapıları için dalga aşması tahmini sonuçları elde edebilmektedir. Bu araç, taş dolgulu yapılar ve kıyı duvarları yapılarında dalga aşması tahminlerini hesaplayabilmektedir. Ancak kordon, durgun dalga havuzu ile bütünleşik kıyı duvarlarında dalga aşması hesaplaması yapamamaktadır. Durgun dalga havuzu ile bütünleşik kıyı duvarları özellikle rekreasyonel aktivitelerin yoğun yapıldığı alanlarda verimli bir kıyı koruma uygulamasıdır. Bu yapılar küçük dalga aşması değerlerini daha küçük kret seviyeleri ile elde etmelerinden ötürü, verimli bir kıyı koruma örneğidirler.

Bu çalışmada durgun dalga havuzu ile bütünleşik kıyı duvarlarında dalga aşması yapabilen yeni bir YSA aracı geliştirilmiştir. YSA aracının eğitim ve testi için veri tabanı oluşturulmuştur. En uygun yapay sinir ağları modeli mimarisi analiz edilmiş olup en uygun parametreler Grid Search metodu ile seçilmiştir. Yeni oluşturulan bu

yapay sinir ağları modelinin performansı literaturdeki empirik formüllere ve EurOtop (2018) tarafından önerilen Overtopping-Neural Network yapay sinir ağları modeline karşı değerlendirilmiştir.

Yeni oluşturulan yapay sinir ağları modeli hem dik kıyı duvarlarında hem de dalga havuzu ile bütünleşik kıyı duvarlarında yüksek doğruluk performans değerleri elde etmiştir. Bu çalışmada oluşturulan yeni yapay sinir ağları modeli dik kıyı duvarlarında Overtopping-Neural Network modeline ve literatürdeki ampirik formüllere göre daha iyi bir performans göstermiştir. Durgun dalga havuzu ile bütünleşik kıyı yapılarında ise literatürdeki ampirik formüller ile yakın bir performana sahiptir.

Anahtar Kelimeler: Dalga Aşması, Makine Öğrenmesi, Yapay Sinir Ağları, Durgun Dalga Havuzu

To my mother, Hava Uzun Paşaoğlu

ACKNOWLEDGMENTS

I am thankful my supervisor Assist. Prof. Dr Gülizar Özyurt Tarakcıoğlu for her all support and guidance. She supported my idea of thesis and her previous studies became a solid foundation for my thesis. In addition, Assoc. Assist. Prof. Dr Doğan Kısacık's studies and knowledge make this thesis to be finished well.

I am thankful to my girlfriend Seher Aytüre for keeping my desire to finish this thesis high with threats and violence.

I am thankful to my family for all their support both in moral and physical. They are always patient and respectful my such long education journey.

I am very grateful to my all team members of METU Orienteering and Navigation Team. Both orienteering and this team make my whole education and master journey joyful and bearable.

I am thankful to Prof. Dr. Lorenzo Cappietti for sharing experiment test results of his study.

TABLE OF CONTENTS

ABSTRACT v

ÖZ vii

ACKNOWLEDGMENTS x

TABLE OF CONTENTS xi

LIST OF TABLES xiv

LIST OF FIGURES xv

CHAPTERS

1 INTRODUCTION 1

1.1 Motivation 1

1.2 Objectives of the Study 2

1.3 Chapters of the thesis 3

2 LITERATURE REVIEW 5

2.1 Wave Overtopping on Vertical Walls 5

2.2 Wave Overtopping on Vertical Walls with SWB and its superstructures 8

2.2.1 Promenade 9

2.2.2 Storm Wall 9

2.2.3 Bullnoses 10

2.2.4 Stilling Wave Basin 12

2.3 Artificial Neural Networks for Wave Overtopping 17

3 METHODOLOGY 21

3.1 Datasets Used 21
3.1.1 Extended CLASH Database 22
3.1.2 Overtopping Experiments of Vertical Seawall and SWB combinations at METU, Turkey 23
3.1.3 Composite Vertical Seawall Tests in LABIMA, Italy 24
3.1.4 Final Database Created 24
3.2 Input and Target Parameters 27
3.2.1 Raw Parameters 27
3.2.2 Scaling Features 30
3.3 The ANN Architecture 31
3.3.1 The Feedforward Propagation Algorithm 32
3.3.2 Backpropagation Algorithm 34
3.3.3 Hyper parameter selection 37
3.3.4 Train, cross validation and test splitting 41
3.4 Model Evaluation 42
3.4.1 Learning curves 42
3.4.2 Domain Validity Check 42
3.4.3 Accuracy metrics 43
3.4.4 Literature Empirical Formulas 43
3.5 Software Used 43
4 RESULTS and DISCUSSION 45
4.1 Grid Search Results 45
4.2 Learning Curves 47
4.3 Domain Validity of the New Neural Network 47

4.4 Accuracy metrics 49
4.4.1 EU_VER Test Dataset.....51
4.4.2 METU_VER Test Dataset.....53
4.4.3 METU_SWB Test Dataset 55
4.4.4 LABIMA_SWB Test Dataset.....57
5 CONCLUSIONS.....59
REFERENCES
APPENDICES 63
A. Grid Search Results for each Hyper-parameter Combination 63

LIST OF TABLES

TABLES

Table 2.1 Coefficients of reduction factor for each schema tested in METU 15
Table 2.2 Coefficients of reduction factor for each schema tested in LABIMA..... 16
Table 3.1 Labels for the physical test in the Extended CLASH database 22
Table 3.2 Core data attribute for the physical test in the Extended CLASH database 23
Table 3.3 Parameters of the new vertical wall with superstructures database 25
Table 3.4 Dataset characteristics 26
Table 3.5 Selected input parameters for the ANN 28
Table 3.6 Input value overviews 30
Table 3.7 Hyperparameters Grid 40
Table 3.8 Test portions for each dataset 41
Table 4.1 Best results for the vertical wall ANN 45
Table 4.2 Selected Hyper-parameters..... 46
Table 4.3 Accuracy of the predictions according to models 49
Table A.1 Grid search results 63

LIST OF FIGURES

FIGURES

Figure 2.1. A mound in front of the vertical wall (EurOtop, 2018)..... 6
Figure 2.2. Vertical wall crest modification superstructures (Kısacık et al., 2022) . 8
Figure 2.3. Bullnose schematization (EurOtop, 2018) 11
Figure 2.4. Basic representation of SWB (EurOtop, 2018) 12
Figure 2.5. Overspill basin used in the study of Crema et al. (2009) 13
Figure 2.6. Kısacık et al. (2019) specified SWB schema (a: side view, b:top view) 14
Figure 2.7. Schema xi of the METU SWB on vertical wall experiments (Kısacık et al., 2022) 15
Figure 2.8. C6 schema tested in LABIMA (Kısacık et al., 2022)..... 16
Figure 2.9. Parameters used for the NN-modelling of wave overtopping discharges. 17
Figure 3.1. Final database parameter schema 26
Figure 3.2. An example of a Neural Network with one hidden layer and three nodes 33
Figure 3.3. Gradient descent algorithm (Pedregosa et al., 2011)..... 36
Figure 3.4. Error produced from model with different complexities. Blue curves indicate the training error and red curves indicates the test error Hastie et al. (2009) 39
Figure 4.1. $R2$ heat map of hidden layer sizes and alpha hyper-parameters candidates 46
Figure 4.2. Learning curve of selected vertical wall ANN tool..... 47
Figure 4.3. Training measured and test prediction wave overtopping values scatter plot 48
Figure 4.4. EU_VER dataset non-dimensional wave overtopping values (solid line: prediction equal to measured rate, dashed lines: prediction equal to 10 times higher and lower than the measured rate) 51

Figure 4.5. EU_VER dataset prediction error ratios of non-dimensional wave overtopping values.....52
Figure 4.6. METU_VER dataset non-dimensional wave overtopping values (solid line: prediction equal to measured rate, dashed lines: prediction equal to 10 times higher and lower than the measured rate).....53
Figure 4.7. METU_VER prediction error ratios of non-dimensional wave overtopping values.....54
Figure 4.8. METU_SWB dataset non-dimensional wave overtopping values (solid line: prediction equal to measured rate, dashed lines: prediction equal to 10 times higher and lower than the measured rate).....55
Figure 4.9. METU_SWB prediction error ratios of non-dimensional wave overtopping values.....56
Figure 4.10. LABIMA_SWB dataset non-dimensional wave overtopping values (solid line: prediction equal to measured rate, dashed lines: prediction equal to 10 times higher and lower than the measured rate).....57
Figure 4.11. LABIMA_SWB ratios error percentage of non-dimensional wave overtopping values.....58

CHAPTER 1

INTRODUCTION

1.1 Motivation

Coastal zones are highly populated and urbanized areas. They are inhabited by most of the people in the world and hold many resources for people. However, they are vulnerable to coastal hazards such as overtopping, storm surges and coastal flooding. Moreover, due to sea level rise, the vulnerability of this coastal hazards will be increased. Zerbini et al. (2017) measured the yearly mean sea-level rise as 1.3mm/year between 19th century and 2012. Currently, this sea level rise accelerated due to global climate change. This situation leads the coastal instructions and engineers to develop innovative coastal protection systems and update existing structures.

Vertical walls and dikes are common sea defense structures. Since their design criteria depend on sea characteristics such as water levels, waves, and tides, their design has to adapt to increase of coastal vulnerabilities. Among the criteria, the wave overtopping value is the main performance criteria to design for flood protection.

Increasing the crest height is one of the common adaptation methods in order to decrease wave overtopping values on vertical walls and sea dikes. However, coastal zones are highly recreational areas and sea scenery may be important and increasing crest height is limited for these locations (Kısacık et. al, 2022). Combining vertical wall with different kind of superstructures are used to adapt vertical wall to critical water level and wave conditions without increasing crest height. These structures are promenades with slope, seaward and landward storm walls, bullnoses and stilling wave basins (SWB).

Kısacık et al. (2019) analyzed the performance of the SWB on seawall of Izmir by physical modelling and offers an optimized vertical wall with SWB for this location. In addition, Kısacık et al. (2022) analyzed individual influence of vertical wall superstructures and SWB on vertical wall on the wave overtopping values. Although, the experiments of the Kısacık et al. (2022) study contains many wave conditions and superstructure geometries, proposed wave overtopping empirical formulas are valid only for specific type of geometries and under given wave conditions. Further experiments are to generalize these formulas.

Designing vertical wall with superstructures and SWB with desired geometry by using physical models would be much time and money consuming. On the other hand, the artificial neural networks (ANN), are practical to use and after training process, making predictions doesn't take much time. In addition, once they are trained with a large enough database, they are capable of representing the wave dynamics (Zanuttigh and Formentin 2016).

EurOtop (2018) adopted an artificial neural network, The Overtopping-Neural Network tool, for the prediction of wave overtopping at sea defense structures. In order to train this model Crest Level Assessment of Coastal Structures (CLASH) database and some extra physical test results were used. Although the model can predict wave overtopping values at 6 different kind of sea defense structures, it cannot be used when calculating wave overtopping at vertical walls containing SWB and its superstructures. Input values and schema of The Overtopping-Neural Network tool doesn't contain SWB and its related parameters. A method for wave overtopping prediction on vertical wall with SWB and its superstructures is the literature gap aimed to be filled in this thesis.

1.2 Objectives of the Study

In this thesis, creation of a new artificial neural network is aimed to calculate the wave overtopping on vertical walls with SWB and similar superstructures. New database is created in order to train this new ANN tool by combining train data of

The Overtopping-Neural Network and of Kısacık et al. (2019) and (2022) physical test results. The Overtopping-Neural Network input parameters are updated in order to cover SWB and its superstructure geometries. The performance of new ANN tool is tested against existing empirical formulas and The Overtopping-Neural Network.

1.3 Chapters of the thesis

This thesis consists of 4 main chapters except the current introduction section.

In the second chapter, literature studies about wave overtopping on vertical walls with SWB and its superstructures are summarized. In addition, the artificial neural networks used in wave overtopping prediction is presented.

In the third chapter methodology used for the creation of the new neural network and evaluation of the neural network is presented. This chapter includes 5 parts. The first part includes collection and creation of the new database. The second part contains the selection of the input parameters of the new ANN tool. The third part gives general information on how neural network tool works and the architecture of the neural networks. The fourth part provides information about how created model is evaluated against existing methods and the final part presents the software used in order to create and use the new ANN tool.

In the fourth chapter, obtained results and discussion of these results are presented in detail highlighting the performance of the new ANN tool.

In the fifth chapter, conclusion of the study is presented. In addition, further studies are proposed in this chapter.

Finally, ANN tool parameters and their performance metrics are tabulated as the Appendix chapters.

CHAPTER 2

LITERATURE REVIEW

In this chapter, previous studies which provides a background to this thesis study are presented. In this thesis, wave overtopping on vertical wall and vertical walls with stilling wave basins and its superstructures and calculation of the wave overtopping value by using artificial neural networks is investigated. In this part, the literature studies of wave overtopping on vertical walls, stilling wave basins, promenades, storm walls with bullnoses crest modification superstructures and their influence on wave overtopping and artificial neural networks used in wave overtopping calculation is summarized.

2.1 Wave Overtopping on Vertical Walls

Wave overtopping calculations on vertical walls are summarized in EurOtop (2018). According to EurOtop (2018), wave overtopping discharge on vertical wall depends on if there is influence of the foreshore in front of the structure, if there is impulsive overtopping condition and if there is a mound in front of the structure. The final conditions classify vertical wall as a composite vertical wall or a plain vertical wall.

The foreshore slope may have affected the individual waves approaching the structure. The bathymetry may change wave shoaling, refraction and the breaking behavior of individual waves and this process called as influencing foreshore (EurOtop 2018). If there are intermediate and shallow wave conditions and also foreshore slope values are 1:50 and steeper, influencing foreshore can be stated in the region. In the absence of the influencing foreshore EurOtop (2018) suggests following equations.

$$\frac{q}{\sqrt{g * H_{mo}^3}} = 0.0047 * \exp\left(-\left(2.35 * \frac{R_c}{H_{mo}}\right)^{1.3}\right) \qquad 2.1$$

$$\frac{q}{\sqrt{g * H_{mo}^3}} = 0.0054 * \exp\left(-\left(2.12 * \frac{R_c}{H_{mo}}\right)^{1.3}\right) \qquad 2.2$$

The 2.1 can be used in predictions and comparisons with measurements and 2.2 can be used in design and safety assessments.

In the presence of a mound in front of the structure, treating structure as a vertical wall or composite vertical wall decision has to be made. The Figure 2.1 shows vertical wall schema with a mound in front of it. In order to say there is influence of the mound, water depth above the toe of the vertical wall must be lower than the 60 percent of the water depth at the structure toe (Van der Meer and Bruce, 2014).

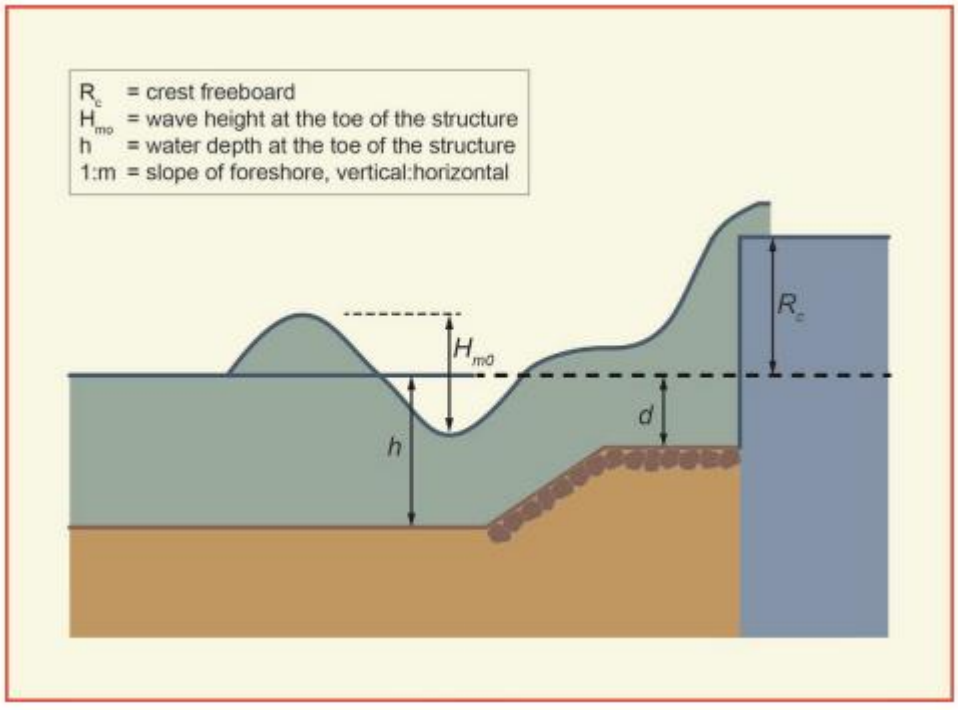


Figure 2.1. A mound in front of the vertical wall (EurOtop, 2018)

The final check is if there are impulsive wave conditions which may lead breaking wave on the vertical wall. This impulsiveness criteria changes with if the vertical wall is composite or plain vertical wall. In the conditions stated in 2.3 and 2.4 there is no impulsive wave conditions.

$$h^2/(H_{m0} * L_{m-1,0} < 0.23 \qquad d/h \leq 0.6 \qquad 2.3$$

$$h^2/(H_{m0} * L_{m-1,0} < 0.65 \qquad d/h > 0.6 \qquad 2.4$$

If there are no impulsive conditions the 2.5 can be used to predict wave overtopping values. 2.6 can be used to calculate wave overtopping values in design and safety purposes.

$$\frac{q}{\sqrt{g * H_{mo}^3}} = 0.05 * \exp(-2.78 * R_c/H_{m0}) \qquad 2.5$$

$$\frac{q}{\sqrt{g * H_{mo}^3}} = 0.062 * \exp(-2.61 * R_c/H_{m0}) \qquad 2.6$$

If there are impulsive wave conditions for plain vertical wall Equation 2.7 can be used for prediction of the wave overtopping values on lower non dimensional relative freeboard values ($0 < R_c/H_{mo} \leq 1.35$) and Equation 2.8 can be used for the higher non dimensional relative freeboard values, $R_c/H_{m0} > 1.35$.

$$\frac{q}{\sqrt{g * H_{mo}^3}} = 0.011 * \left(\frac{H_{m0}}{h * s_{m-1,0}}\right)^{0.5} * exp(-2.2 * \frac{R_c}{H_{m0}}) \qquad 2.7$$

$$\frac{q}{\sqrt{g * H_{mo}^3}} = 0.0014 * \left(\frac{H_{m0}}{h * s_{m-1,0}}\right)^{0.5} * \left(\frac{R_c}{H_{m0}}\right)^{-3} \qquad 2.8$$

If there are impulsive wave conditions for composite vertical wall Equation 2.9 can be used for prediction of the wave overtopping values on lower non dimensional relative freeboard values ($0 < R_c/H_{mo} \leq 1.35$) and Equation 2.10 can be used for the higher non dimensional relative freeboard values, $R_c/H_{m0} > 1.35$.

$$\frac{q}{\sqrt{g * H_{mo}^3}} = 1.3 * \left(\frac{d}{h}\right) * 0.011 * \left(\frac{H_{m0}}{h * s_{m-1,0}}\right)^{0.5} * exp(-2.2 * \frac{R_c}{H_{m0}}) \quad 2.9$$

$$\frac{q}{\sqrt{g * H_{mo}^3}} = 1.3 * \left(\frac{d}{h}\right) * 0.0014 * \left(\frac{H_{m0}}{h * s_{m-1,0}}\right)^{0.5} * \left(\frac{R_c}{H_{m0}}\right)^{-3} \quad 2.10$$

2.2 Wave Overtopping on Vertical Walls with SWB and its superstructures

Sea defense structures may have some superstructures to control transmission of the waves and decrease wave overtopping discharges. These superstructures are at the top of the sea defense structure. Their shape and sizes have influence on the wave overtopping. These superstructures are promenades with slopes, storm walls, bullnoses and SWB which is a combination of all others. The influence of the structures is represented as reduction factors for occurrence of each structure. These reduction factors exerted on R_c/H_{m0} term and updates this part of the wave overtopping equations mentioned in section 2.1 as $\frac{R_c}{H_{m0}} * \frac{1}{\gamma^*}$. The reduction factors are obtained by physical test results by comparing overtopping discharge calculated with original formulas with the discharge values measured for the cases with superstructures (Kısacık et al., 2022). Figure 2.2 show possible crest superstructures that can be added to vertical walls.

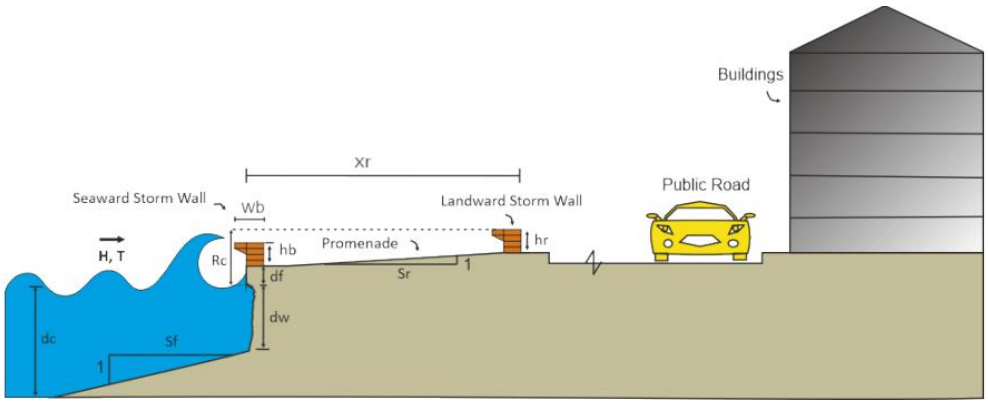


Figure 2.2. Vertical wall crest modification superstructures (Kısacık et al., 2022)

2.2.1 Promenade

Promenades are horizontal part at the landward direction of a sea defense structure. It usually placed 5-25 meters long and having 1% to 2% slopes. The longer promenades lead lower wave overtopping values at the end of the promenade (Kısacık et al., 2022). The Equation 2.11 is provided in EurOtop (2018) for the calculation of the reduction factor of promenades for dikes for relative promenade ($\frac{X_r}{L_{m-1,0}}$) length between 0.05 and 0.5. There is no formula provided for promenade reduction factor on vertical walls.

$$\gamma_{prom} = 1 - 0.47 * \frac{x_r}{L_{m-1,0}} \quad 2.11$$

2.2.2 Storm Wall

Storm walls can be used on the vertical wall or also at the end of the promenade as a landward storm wall. Seaward storm walls wave overtopping calculations exists on EurOtop (2018), but landward storm wall wave overtopping formulas doesn't exist on EurOtop (2018). However, there is some studies on landward storm walls on dikes in the literature.

Tuan (2013) has suggested a formulation of a reduction factor for landward storm walls at the end of the promenade in sea dikes. This reduction factor is multiplication of two reduction factor corresponding promenade and storm wall height. The reduction factor calculated with following formulas.

$$\gamma_{prom_v} = \gamma_v * \gamma_{prom} \quad 2.12$$

$$\gamma_v = \frac{1}{1 + 1.60 * \frac{h_b}{R_c * \zeta_{0m}}} \quad 2.13$$

$$\gamma_{prom} = \frac{1}{1 + \frac{1}{8} * \frac{x_r}{H_{m0} * \zeta_{0m}}} \quad 2.14$$

ζ_{m0} is Iribarren number calculated with spectral wave period, x_r is the promenade width.

Van Doorslaer et al. (2015), updated the formula of Tuan (2013). In this new formulation γ_{prom} calculated as equation 2.11 and updated γ_v and γ_{prom_v} as follows.

$$\gamma_v = \exp(-0.56 * \frac{h_b}{R_c}) \quad 2.15$$

$$\gamma_{prom_v} = 0.87 * \gamma_v * \gamma_{prom} \quad 2.16$$

Zanuttigh and Formentin (2018) studied wave overtopping on sea dikes with promenades and landward storm walls. They updated formula with a breaking parameter ($\xi_{m-1,0}$).

$$\gamma_{prom_v} = \gamma_{prom_v} / \tanh(\xi_{m-1,0}) \quad 2.17$$

2.2.3 Bullnoses

Bullnose is an extension towards to sea, placed on crest of the sea defense structure. This extension leads sea waves to move back to sea and therefore decrease the wave overtopping value. The Figure 2.3 shows a bullnose schema. This principle introduced firstly in studies of Goda (1985) and Franco (1994). Van Doorslaer and De Rouck (2010) suggested static reduction factor value as 0.7.

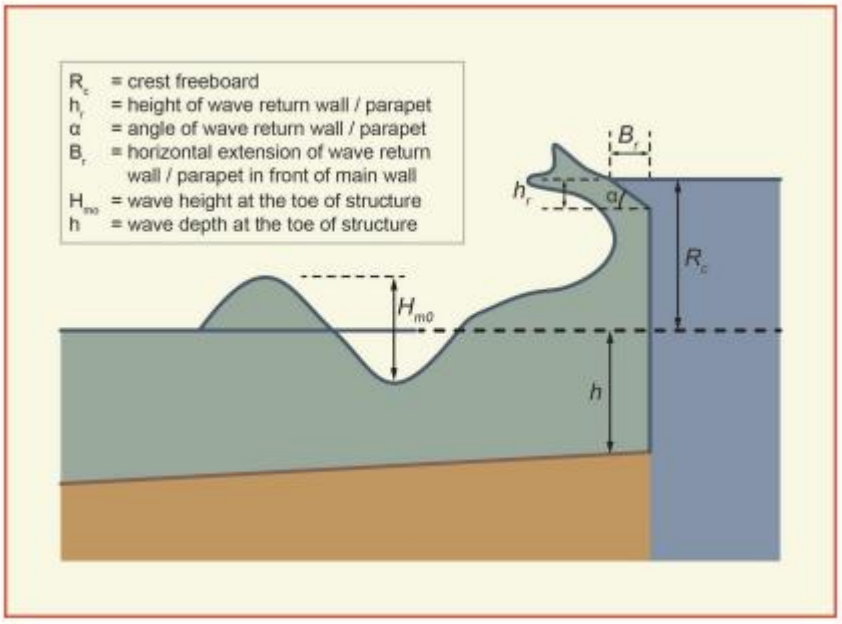


Figure 2.3. Bullnose schematization (EurOtop, 2018)

EurOtop (2018) suggests following formulas for calculation of bullnose reduction factors on seawalls.

$$\gamma = 1.0 \qquad R_c/H_{m0} \leq 0.5 \qquad 2.18$$

$$\gamma = 1.3 - 0.6 * R_c/H_{m0} \qquad 0.5 < R_c/H_{mo} \leq 1.0 \qquad 2.19$$

$$\gamma = 0.7 \qquad R_c/H_{mo} > 1.0 \qquad 2.20$$

Martinelli et al. (2018) done physical tests with vertical walls with bullnoses and verified Eurotop 2018 equations. Van Doorslaer et al. (2015) studied dikes with bullnoses and other crest modification superstructures. Zanuttigh and Formentin (2018) extended these studies with breaking waves. This study analyses the combined effects of this superstructures when they are used at the same time on dikes.

2.2.4 Stilling Wave Basin

Stilling wave basins (SWB) defined as crest structures that has a partially permeable storm wall at sea side and a storm wall at landward at a sea defense structure. (Eurotop, 2018). Both these walls can contain bullnoses and mainly they have promenade in between. In Figure 2.4. Basic representation of SWB structure main schema is represented.

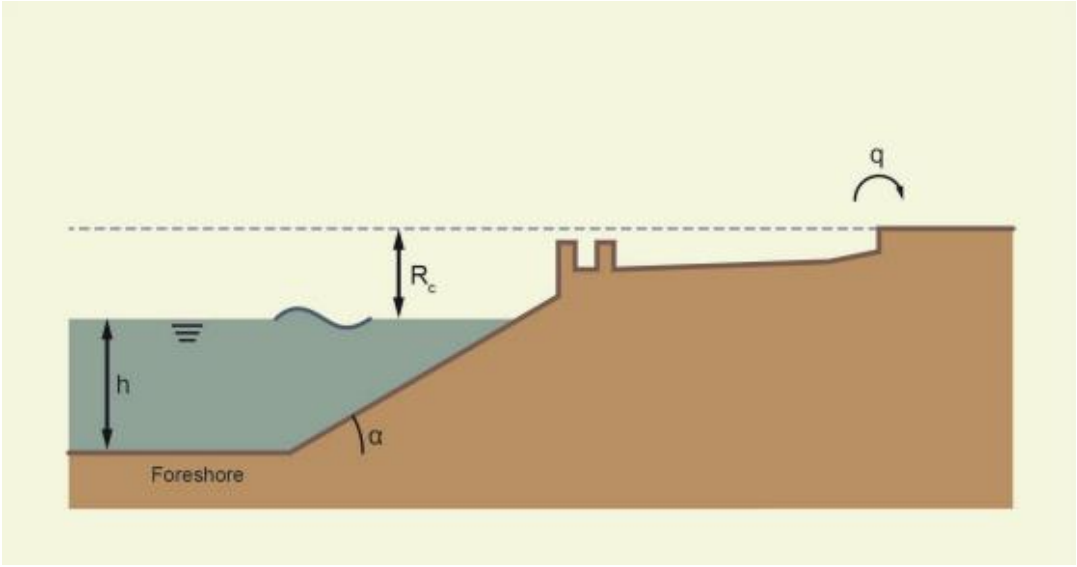


Figure 2.4. Basic representation of SWB (EurOtop, 2018)

Di Risio et al. (2006) discussed SWB performance on wave overtopping with physical tests. They tested structure named as Overspill basin and this structure contains a seaward storm wall promenade and a landward storm wall with a parapet at the end of the promenade. The Figure 2.6 shows an Overspill basin example. They had done 2-D physical tests in non-braking wave conditions. They observed lower wave overtopping discharges with Overspill basin design.

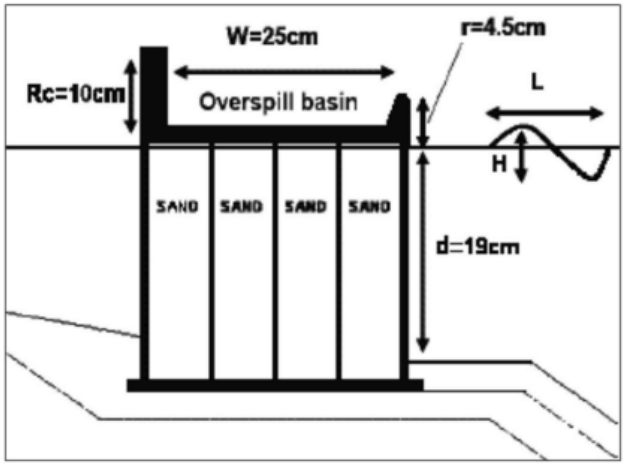


Figure 2.5. Overspill basin used in the study of Crema et al. (2009)

Crema et al. (2009), also conducted a laboratory study on also Overspill basin on a plain vertical wall. He proposed a formula include this structure as a reduction factor. γ_{SWB} taken as 0.69 in this equation for relative freeboard ranges of 1.18 and 1.85.

$$\frac{q}{\sqrt{g * H_{mo}^3}} = 0.04 * \exp\left(-\left(2.6 * \frac{R_c}{H_{mo}} * \frac{1}{\gamma_{SWB}}\right)^{1.3}\right) \qquad 2.21$$

Kısacık et al. (2019) analyzed vertical walls with SWB structure. They discussed different kind of SWB combinations together and discussed their efficiency. They proposed new γ_{SWB} values for a specified type of vertical wall with SWB. This specified geometry shown in the Figure 2.6. The Equation 2.22 and Equation 2.23 the γ_{SWB} values for low freeboard and high freeboard conditions.

$$\gamma_{SWB_low} = -0.0615 * \frac{R_c}{H_{m0}} + 0.577 \qquad 0.708 < R_c/H_{m0} \leq 1.35 \qquad 2.22$$

$$\gamma_{SWB_high} = -0.3812 - \frac{R_c}{H_{m0}} + 0.828 \qquad 1.35 < R_c/H_{mo} \leq 2.09 \qquad 2.23$$

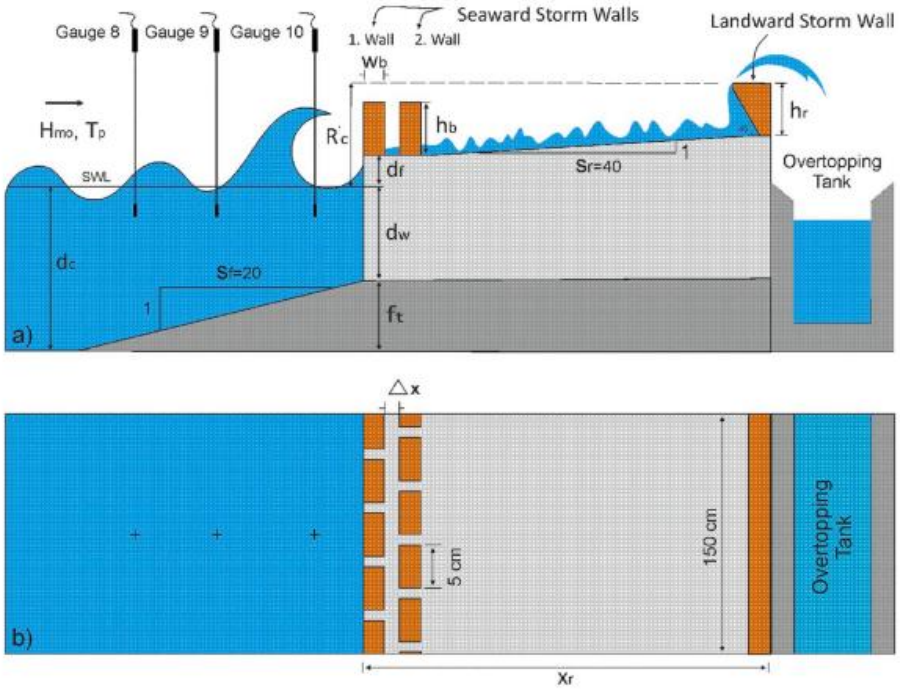


Figure 2.6. Kısacık et al. (2019) specified SWB schema (a: side view, b:top view)

Kısacık et al. (2022) conducted several physical experiments in Coastal Engineering Laboratory, Middle East Technical University (METU-Turkey) and LABIMA, the Maritime Engineering Laboratory of the Civil Engineering Department of Florence University (Italy). In METU they studied 9 vertical walls with different SWB schema and 3 composite vertical walls with different SWB schema for LABIMA. They calculated new γ_{SWB} values for all the SWB schemas.

In METU, schema i contains only a promenade. Schema ii contains a seaward continuous storm wall with parapet and a promenade. Schema iii contains a landward continuous storm wall without parapet and a promenade. Schema iv contains a landward storm wall with a parapet and a promenade. Schema v contains double row SWB as a seaward storm wall, a landward continuous storm wall without a parapet and a promenade. Schema vi contains a double row SWB as a seaward storm wall, a continuous storm wall with parapet a promenade. Schema vii contains a double row SWB as a seaward storm wall with a parapet, a continuous landward storm wall without a parapet and a promenade. Schema viii contains double row SWB with a

parapet as seaward storm wall and a continuous landward storm with a parapet and a promenade. Schema ix contains a single row SWB with a parapet as a seaward storm wall, continuous landward storm wall with a parapet and a promenade. Figure 2.7 represents schema viii and this schema contains all kind of superstructures tested in the study.

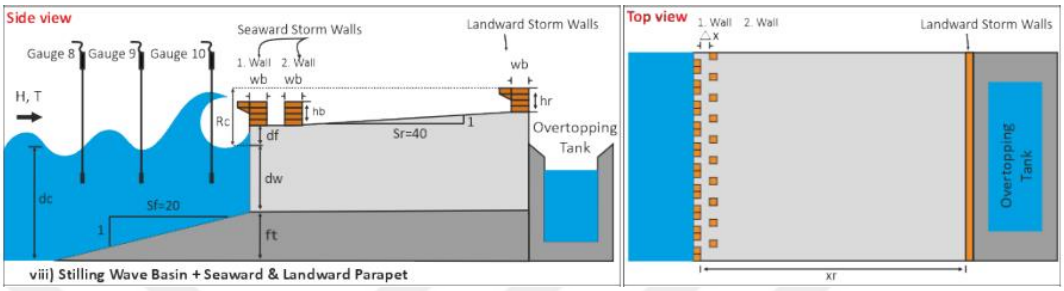


Figure 2.7. Schema xi of the METU SWB on vertical wall experiments (Kısacık et al., 2022)

The reduction factor calculated with respect to equation 2.24 and equation 2.25 according to corresponding k, l, m and n values shown in the Table 2.1.

$$\gamma_{SWB_low} = k - l * R_c/H_{mo} \quad 2.24$$

$$\gamma_{SWB_high} = m - n * R_c/H_{mo} \quad 2.25$$

Table 2.1 Reduction factor calculated tested in METU (Kısacık et al., 2022)

Type	*k*	*l*	*m*	*n*
i	1.0252	0.0580	1.5039	0.4028
ii	1.1932	0.4502	1.7648	0.8954
iii	0.6757	0.0053	0.8664	0.2245
iv	0.7166	0.0674	1.1491	0.4767
v	0.6414	0.0170	0.8113	0.2471
vi	0.6439	0.0383	0.7501	0.2577
vii	0.6895	0.1618	-	-
viii	0.655	0.1569	-	-
ix	0.7454	0.2139	-	-

LABIMA test experiment composite wall with SWB schemas named as C5, C6 and C8. C5 has a landward storm with narrow promenade. C8 has also a landward storm wall but with wider promenade. C6 has a landward storm wall with narrow promenade and also a single row SWB as a seaward storm wall. Figure 2.8 represents C6 and this schema has all superstructures tested at LABIMA. Table show k, l, m and n values for the calculation of the reduction factors for each schema.

Table 2.2 Coefficients of reduction factor for each schema tested in LABIMA (Kısacık et al., 2022)

Type	*k*	*l*	*m*	*n*
C5	0.1466	0.5730	-	-
C6	0.2099	0.4562	-	-
C8	0.1766	0.4661	-	-

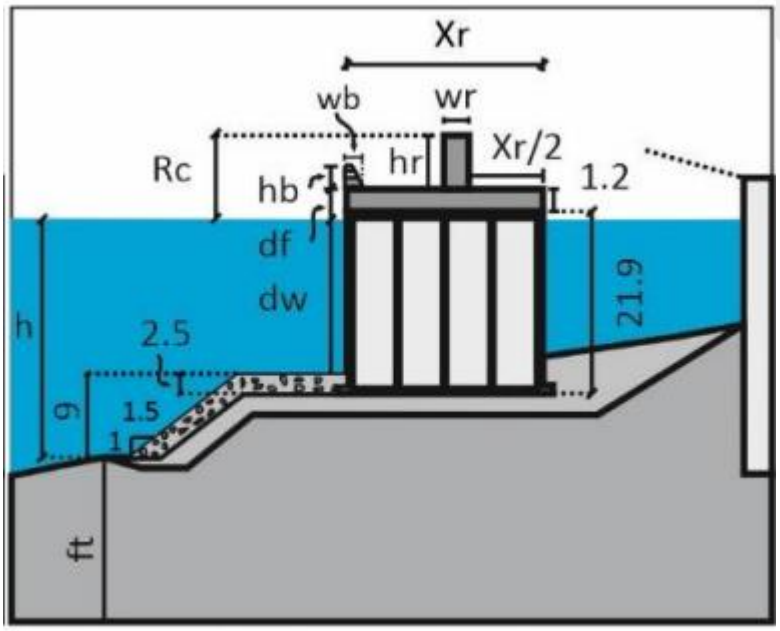


Figure 2.8. C6 schema tested in LABIMA (Kısacık et al., 2022)

2.3 Artificial Neural Networks for Wave Overtopping

Neural network studies on the wave overtopping started with Crest Level Assessment of Coastal Structures (CLASH) project. This project had two main objectives. The first one was the analyze scale effects on wave overtopping values measured on prototype physical models. The second one was to collect a huge database and use this database to create an artificial neural network model (ANN) which can calculate wave overtopping on sea defense structures. Van Gent et al. (2007) developed the first wave overtopping ANN model. 10 000 data used for training and test purposes of the ANN. This ANN consists of 14 input neurons and 20 neurons in the hidden layer. All input parameters are presented in Figure 2.9. This neural network can't calculate zero wave overtopping values.

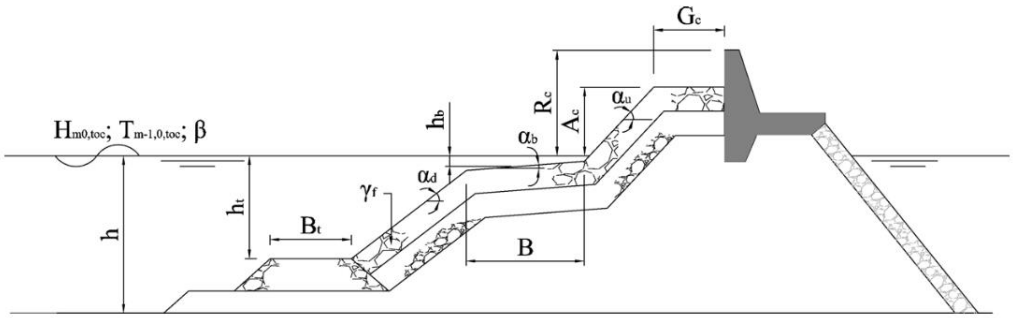


Figure 2.9. Parameters used for the NN-modelling of wave overtopping discharges.

In this study, in order to overcome scale effects between different kind of tests Froude's similarity law is used and each data scaled according $H_{m,0,toe} = 1\ m$ (Van Gent et al., 2007).

In order to generalize and obtain accurate results for each type of sea defense structure, resamples technique is applied in training and testing. Each evaluation score for training calculated is as mean of N different training process' results. For each N process, different portion of the data is used. In this study, N is taken as 500 for training purposes and 50 for determining neural network architecture purposes (Van Gent et al., 2007). This model and following all studies used same training

algorithm of $Levenberg - Marquardt$ algorigtm and *hyperbolic tangent sigmoid* function as hidden neurons transfer function.

Verhaeghe et al. (2008) developed a new ANN model. This ANN model has two phases. In the first phase, ANN predicts if there is wave overtopping or not, and in the second phase, it predicts the value of log scaled wave overtopping discharge. This ANN model has 13 inputs parameters. 20 hidden neurons used in hidden layer of the first phase and 25 hidden neurons are used in hidden layer of the second phase.

Later, Zanuttigh et al. (2013) studied the existing ANN models of wave overtopping and created a new ANN model for the prediction of wave reflection (K_r) and wave transmission (K_t) values. Zanuttigh et al. used 13 non dimensional input parameters for this ANN model and 40 neurons in the hidden layer of the model.

Zanuttigh et al. (2014) extended the CLASH database and used this database to create a new wave overtopping ANN model. This new model can calculate wave overtopping, wave reflection and wave transmission values on sea defense structures. In this study, usage of non-dimensional inputs is analyzed by comparing the new ANN model with Van Gent et al.'s (2007) ANN model. According to this study, non-dimensional inputs show better performance and 15 non-dimensional input parameters are used in this ANN model. 40 hidden neurons are used in the hidden layers of the neural network.

Zanuttigh et al. (2016) optimized the ANN model again. In this study, they also work with a two phased neural network like Verhaeghe et al. (2008) to calculation of wave overtopping discharge and classify a structure as overtopping occurs and overtopping doesn't occur. The ANN model is also tested against physical tests which the data was not included in the training phase.

Formentin et al. (2017) summarized their previous studies of Zanuttigh et al. (2013), Zanuttigh et al. (2014) and Zanuttigh et al. (2017), and offered the final ANN model. They created the final version of the ANN model and this model is delivered upon registration at www.unibo.it/overtopping-neural network. The model contains 15

non-dimensional input parameters and 20 hidden neurons in hidden layers. This model is also adopted by EurOtop (2018).

Formentin and Zanuttigh (2017) defined methodological approach for developing and testing of artificial neural network based solution for wave-structure interaction processes. In this study, they mentioned about methods for database creation, input parameter selection and training phases of the ANN models. The study also contains information on test metrics that can be used to evaluate wave-structure interaction ANN models.

CHAPTER 3

METHODOLOGY

In this chapter, selection of input parameters, the datasets used, details of improved ANN for vertical wall structures and developed ANN for vertical wall with SWB super structure and its components are described. Additionally, the tool used to develop ANN structure (Scikit-learn) is described and introduced.

3.1 Datasets Used

In this study, datasets from three independent research are combined for the modeling of artificial neural network to predict wave overtopping on vertical seawalls and SWB components. The first dataset is the extended CLASH database by Formentin et. al (2017) which is used to develop The Overtopping-Network tool adopted by EurOtop Manual (2018). The second dataset is the experimental data of Kisacik et al (2019, 2022) that tested the overtopping at a representative urban seawall under a range of hydrodynamic conditions encompassing those conditions of inner Bay of Izmir. These tests included both simple vertical seawall as well as cases with stilling wave basin superstructure and its components. The final dataset belongs to another experimental work where SWB elements on a composite vertical seawall in Italy were evaluated at a wave-current flume of LABIMA, the Maritime Engineering Laboratory of the Civil Engineering Department of Florence University (Italy) (Kisacik et al. 2022). The details of these datasets and the range of variables are presented in the following section.

3.1.1 Extended CLASH Database

Formentin et al. (2017) extended the CLASH database which is used in order to obtain ANN tool for wave overtopping estimation (Van Gent, 2007). Data is collected from available literature work, starting with original datasets but reorganized to follow the schematization of The Overtopping-Neural Network tool adopted by EurOtop (2018). This database has 17,942 test results and data contains 14 hydraulic and 23 structural parameters and 4 general parameters such as reliability and complexity factors, and an indication of test usage in training ANN tool (Formentin et al. 2017).

The database contains "Label" attribute for the geometry of the physical tests and "Core Data" attribute for the condition of the physical test affects the usage of the data in creation The Overtopping-Neural Network tool.

Table 3.1 Labels for the physical test in the Extended CLASH database

Label	*Geometry*
A	Rock Permeable
B	Rock Impermeable
C	Amour Units
D	Smooth Slopes
E	Non-straight slopes berms
F	Vertical Wall
G	Oblique Wave Attacks

Table 3.2 Core data attribute for the physical test in the Extended CLASH database

Core Data	*Explanation of the datatype*
Z	Core data; data used for training of the Artificial Neural Network
	Non-core data; tests with specific aspects, not used for the ANN
BN	Structure with a bull nose
D	Double seawall with "basin" in the middle
DH	Structure with drainage holes
C	Tests with currents
PC	Pperforated wall or caisson
RS	Overtopping measured through recirculation system
S	Stepped slope

As this thesis focused on estimating overtopping values in vertical wall structures and superstructures on vertical walls like SWB, only vertical wall data with Label "F" is exported from the Extended CLASH database. Moreover, in order to extract unreliable data, test results with "Z" value of Core Data attribute is used in this study. This portion of data will be called as "EU VER" in following sections.

3.1.2 Overtopping Experiments of Vertical Seawall and SWB combinations at METU, Turkey

In the wave flume of Coastal and Harbor Engineering Laboratory, Middle East Technical University (METU) physical tests were carried out to observe wave overtopping at vertical seawalls (Kisacik, Ozyurt Tarakcioglu, Baykal, 2019) and verticals seawalls with SWB superstructure and its components (Kisacik, Ozyurt Tarakcioglu, Cappietti, 2022). The experiments covered a range of hydrodynamic conditions (26 scenarios of combinations of water depth and wave conditions). The first part of the experiments has 128 data for simple vertical wall structure which is used in this thesis to assess the performance of The Overtopping-Neural Network

tool adopted by EurOtop Manual and to be used as training set for an improved ANN model to predict wave overtopping on vertical seawalls.

The second part of the experiments consists of test on the wave overtopping of a vertical wall combined with different kind of superstructures under the same 26 scenarios of hydrodynamic conditions of the simple vertical wall experiments. The tested superstructures are promenade with slope, seaward storm wall, landward storm wall, storm wall combined with bullnoses and without bullnoses and combination of these components which make the Stilling Wave Basin (SWB). 234 overtopping data was measured in these experiments.

The data taken from Kisacik, Ozyurt Tarakcioglu, Baykal (2019) study will be called as "METU VER" and the data taken from Kisacik, Ozyurt Tarakcioglu, Cappietti (2022) study will be called as "METU SWB" in the following sections.

3.1.3 Composite Vertical Seawall Tests in LABIMA, Italy

The composite vertical wall experimental studies were conducted in the Maritime Engineering Laboratory of the Civil Engineering Department of Florence University which is called LABIMA. The tests are performed under 9 different hydrodynamic conditions. In these studies, 5 different crest modifications for the composite vertical wall were tested. These 5 different crest modifications were combinations of the position of a continuous vertical wall and SWB component. A total number of 180 data was used in this study. This portion of data will be called as "LABIMA SWB" in following sections.

3.1.4 Final Database Created

These 3 datasets used to create a new database created for the purpose of this thesis study. Structural and hydraulic parameters are selected in order to use represent vertical walls with superstructures. Firstly, vertical wall related parameters are taken

from Eurotop ANN database. Then, vertical wall superstructure parameters are taken from physical test studies of Kisacik, Ozyurt Tarakcioglu and Cappietti (2022). The final database consists of 2 hydraulic, 14 structural parameters and 1 general parameter. Table 3.3 show summary for the parameters of the final database.

Table 3.3 Parameters of the new vertical wall with superstructures database

#	*Parameter*	*Unit*	*Type*	*Definition*
1	$H_{m0,t}$	[m]	hydraulic	Spectral wave height at the structure toe
2	$T_{m-1,t}$	[s]	hydraulic	Spectral wave period at the structure toe
3	m	[-]	structural	Foreshore slope
4	h	[m]	structural	Water depth at the structure toe
5	R_c	[m]	structural	Crest height with respect to swl
6	γ_{fd}	[-]	structural	Roughness factor
7	A_c	[m]	structural	Wall height with respect to swl
8	h_t	[m]	structural	Toe submergence
9	x_r	[m]	structural	Promenade width
10	s_r	[-]	structural	Promenade slope
11	w_b	[m]	structural	Seaward storm wall width
12	w_{br}	[m]	structural	Landward storm wall width
13	C_b	[-]	structural	Blocking coefficient
14	Δ_x	[m]	structural	Horizontal gap between the seaward storm walls
15	w_p	[m]	structural	Seaward parapet width
16	w_{pr}	[m]	structural	Landward parapet width
17	db	-	general	Dataset name
18	q	$[m^3/s\ per\ m]$	hydraulic	Wave overtopping

After combining the datasets, the final data is cleaned. Firstly, wave overtopping values with values equals 0 and values lower than $10^{-6}\ m^3/s/m$ is discarded. Since, our model is a regression model calculation float output numbers, calculating for non-overtopping values is not possible. In addition, tests with values lower than $10^{-6}\ m^3/s/m$ is considered as less accurate due to physical test conditions (Van

Gent, 2007). In addition, especially in the EU_VER dataset some experiment values contain negative values of $H_{m0,t}$, h, and T_{m-1t}values. This experiment values also extracted from the database.

The characteristics of the final filtered dataset are listed in the following table.

Table 3.4 Dataset characteristics

	$H_{m0,t}$ (m)	$T_{m-1,t}$ (s)	R_c (m)	q (l/m)	Count
METU SWB	0.0690 - 0.1139	1.2245 - 2.0236	0.0413 - 0.1565	0.0010 - 3.5271	204
METU VER	0.0669 - 0.1139	1.2245 - 2.0236	0.0270 - 0.1430	0.0922 - 3.8505	128
LABIMA SWB	0.0540 - 0.0850	1.1266 - 1.7563	0.0940 - 0.0940	0.0012 - 0.1834	45
EU VER	0.0003 - 0.6027	0.8769 - 7.5000	0.0000 - 1.4600	0.0010 - 14.6000	1739

The database parameters and visualization of the included structural geometries shown in Figure 3.1.

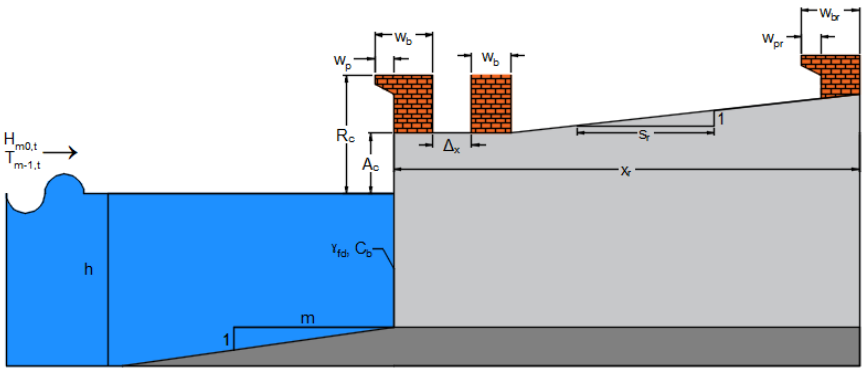


Figure 3.1. Final database parameter schema

3.2 Input and Target Parameters

In this study ANN tools which can calculate wave overtopping of simple vertical wall and vertical wall with different superstructures such as bullnose, promenade, SWB and its components are developed. Wave overtopping is mainly described by deep water wave conditions, wave conditions at the structure and the geometry of the vertical wall structure. Therefore, the input parameters are selected based on the schematization of The Overtopping-Neural Network tool database as well as the geometric descriptors for superstructures included in the thesis. From the Overtopping-Neural Network tool, 8 input parameters are selected to represent the wave parameters and the simple vertical wall geometry. An additional 10 number of parameters are defined to represent the geometry of superstructures. As the number of input parameter increases, ANN becomes more complex and would require larger datasets to achieve better results (Formentin et al., 2017). Therefore, only the parameters related to the objective of the thesis are included in the input parameter set.

3.2.1 Raw Parameters

The datasets used in this thesis are collected from physical tests done in models. Van Gent (2007) scaled these tests according to the Fraud Law by dividing each parameter with the significant wave height, $H_{m0,t}$. This aimed to rescale all test to the same prototype condition which is $H_{m0,t} = 1\ m$. However, Zanuttigh et al. (2014) used non-dimensional parameters in order to exclude different scale conditions. In addition, these 2 processes is compared at the study of the Zanuttigh et al. (2014) and the ANN trained with non-dimensional input parameters gave better results. Therefore, in this thesis non-dimensional parameters are used. All the structure heights became non-dimensional by dividing these values with $H_{m0,t}$ and all structure width became non-dimensional by dividing with the wave length $L_{m-10,t}$. 17 non-dimensional input parameters are given in the following table.

Table 3.5 Selected input parameters for the ANN

#	*Input parameter*	*Type*	*Representation of*
1	$H_{m0,t}/L_{m-1,0,t}$	Wave attack	Wave steepness
2	$h/L_{m-1,0,t}$	Wave attack	Wave shoaling
3	$h_t/H_{m0,t}$	Geometry	Effect of the toe submerge
4	$A_c/H_{m0,t}$	Geometry	Effect of the crest
5	$R_c/H_{m0,t}$	Geometry	Effect of the crown wall
6	m	Geometry	Effect of the foreshore slope
7	γ_f	Structure	Structure roughness
8	$x_r/L_{m-1,0,t}$	Geometry	Promenade width
9	s_r	Geometry	Promenade slope
10	$\Delta_x/L_{m-1,0,t}$	Geometry	Effect of the seawall storm walls gap
11	C_b	Geometry	Blocking coefficient
12	$w_b/L_{m-1,0,t}$	Geometry	Seaward storm wall width effect
13	$h_b/H_{m0,t}$	Geometry	Seaward storm wall height effect
14	$w_{pb}/L_{m-1,0,t}$	Geometry	Seaward parapet effect
15	$w_r/L_{m-1,0,t}$	Geometry	Landward storm wall width effect
16	$h_r/H_{m0,t}$	Geometry	Landward storm wall height effect
17	$w_{pr}/L_{m-1,0,t}$	Geometry	Landward parapet effect

The output parameter is the average wave overtopping discharge. The wave overtopping value became non-dimensional with gravitational acceleration, g and significant wave height at the structure toe value, $H_{m,0,t}$. The average wave overtopping discharge shown in Equation 3.1. The average calculation is the average wave overtopping discharge value across the width of the structure parallel to the sea.

$$q_{AD} = \frac{q}{\sqrt{g * H_{m,0,t}^3}} \qquad 3.1$$

Using and arranging input parameters given in Table 3.5, wave overtopping discharges at plain vertical walls, vertical walls with storm walls with or without parapets, vertical walls with promenades and vertical walls with SWB.

In order to calculate wave overtopping discharges on plain vertical walls, input parameters of $x_r/L_{m-1,0,t}$, s_r , $\Delta_x/L_{m-1,0,t}$, $w_b/L_{m-1,0,t}$, $h_b/H_{m0,t}$, $w_{pb}/L_{m-1,0,t}$, $w_r/L_{m-1,0,t}$, $h_r/H_{m0,t}$ *and* $w_{pr}/L_{m-1,0,t}$ values must be taken as 0.

In order to calculate wave overtopping discharges on vertical walls with storm wall, input parameters of $w_b/L_{m-1,0,t}$, $h_b/H_{m0,t}$, $w_r/L_{m-1,0,t}$, $h_r/H_{m0,t}$ values can be used for the geometry of the both seaward and landward storm walls. Input samples with input parameter of $\Delta_x/L_{m-1,0,t}$ values greater than 0 can be used for double row seaward storm wall and space between them. In addition, $w_{pb}/L_{m-1,0,t}$ and $w_{pr}/L_{m-1,0,t}$ input parameters can be used to include parapet presence in both seaward and landward storm walls. When there is landward storm wall q_{AD} value is the wave overtopping discharge measured behind landward storm wall. Otherwise, q_{AD} value is the wave overtopping value measured behind the seaward storm wall.

In order to calculate wave overtopping values on vertical walls with promenades $x_r/L_{m-1,0,t}$ and s_r input parameters can be used. If there is a promenade in the structures, q_{AD} value is the wave overtopping value measured behind the promenade.

Finally, wave overtopping values at vertical walls with SWB structures estimation can be provided by arranging input parameters discussed for storm walls with or without parapets and promenades.

Overview of the input values according to databases are shown in the Table 3.6.

Table 3.6 Input value overviews

Input Parameter	METU SWB		METU VER		*LABIMA SWB*		*EU VER*	
	min	max	min	max	min	max	min	max
$H_{m0,t}/L_{m-1,0,t}$	0.015	0.033	0.015	0.033	0.014	0.030	0.000	0.087
$h/L_{m-1,0,t}$	0.017	0.081	0.016	0.080	0.057	0.139	0.000	0.666
$h_t/H_{m0,t}$	1.116	2.472	1.084	2.435	0.000	0.000	0.000	22.566
$A_c/H_{m0,t}$	0.279	1.512	0.267	1.910	0.212	1.741	0.000	6.245
$R_c/H_{m0,t}$	0.397	1.954	0.267	1.910	1.106	1.741	0.000	6.245
m	20.000	20.000	20.000	20.000	0.000	7.000	10.000	1050.000
γ_f	1.000	1.000	1.000	1.000	1.000	1.000	0.400	1.000
$x_r/L_{m-1,0,t}$	0.020	0.214	0.000	0.000	0.052	0.126	0.000	0.000
s_r	40.000	40.000	0.000	0.000	0.000	0.000	0.000	0.000
$\Delta_x/L_{m-1,0,t}$	0.000	0.016	0.000	0.000	0.000	0.000	0.000	0.000
C_b	0.000	1.000	1.000	1.000	0.000	0.951	1.000	1.000
$w_b/L_{m-1,0,t}$	0.000	0.013	0.000	0.000	0.000	0.011	0.000	0.000
$h_b/H_{m0,t}$	0.000	0.580	0.000	0.000	0.000	0.407	0.000	0.000
$w_{pb}/L_{m-1,0,t}$	0.000	0.004	0.000	0.000	0.000	0.000	0.000	0.000
$w_r/L_{m-1,0,t}$	0.000	0.013	0.000	0.000	0.005	0.013	0.000	0.000
$h_r/H_{m0,t}$	0.000	0.580	0.000	0.000	0.882	1.389	0.000	0.000
$w_{pr}/L_{m-1,0,t}$	0.000	0.004	0.000	0.000	0.000	0.000	0.000	0.000
q_{AD}	0.00002	0.02966	0.00152	0.03393	0.00003	0.00345	0.00001	8.84802

3.2.2 Scaling Features

Scaling input parameters to a common range is a crucial preprocessing step in machine learning applications. This process involves transforming the input data to a standard scale, typically with a mean of zero and a standard deviation of one. By scaling input parameters to a common range, the machine learning model can more accurately compare and evaluate the importance of different features, as each feature is weighted equally. Scaling also helps to prevent features with larger numerical

values from having an undue influence on the model's output. Furthermore, scaling helps to stabilize the training process and can lead to faster convergence during model training (Singth et al. 2020).

In this study, normalization technique is used. Normalization is a data preprocessing technique, which scales the data to a fixed range between 0 and 1. Specifically, it subtracts the minimum value in each feature and then divides by the range of that feature (i.e., the difference between the maximum and minimum values), resulting in a transformed feature with values between 0 and 1. The 3.2 is used for normalization technique, where X_{mean}, X_{max}, and X_{min} is the minimum, the maximum and the average value of each input parameter used in training of the neural network.

$$X_{scaled} = (X - X_{min}) \,/\, (X_{max} - X_{min}) \qquad 3.2$$

Target or output values are wave overtopping values with units $m^3/sec/m$. Wave overtopping values are extremely small especially in experimental studies therefore firstly these values are logarithmically scaled. Then, like input values, these values are scaled according to 3.2. 3.3 is adopted from Formentin et al. (2017) in order normalize output parameters which is wave overtopping value. This scale process also helps to make model evaluation metrics readable.

$$q_* = \frac{\log(\mathrm{q_{AD}}) - \min(\log(q_{AD}))}{|\min(log(q_{AD})) - \max(\log(q_{AD}))|} \qquad 3.3$$

3.3 The ANN Architecture

Artificial Neural Networks (ANNs) are a type of machine learning model inspired by the structure and function of the human brain. ANNs consist of layers of

interconnected nodes, or neurons, that process input data and generate output predictions.

3.3.1 The Feedforward Propagation Algorithm

The feedforward propagation algorithm is used in neural networks to compute the output of the network for a given input. It involves passing the input data through a series of interconnected layers of neurons, each of which performs a weighted sum of its inputs and applies a non-linear activation function to the result.

3.3.1.1 Hidden Layer Sizes

The hidden layer size defines the nodes numbers and the layers between input and output values. The number of hidden layer and nodes number determines the complexity of the network. Deeper networks with large hidden layers can be useful for high complexity problems, but it requires more data to be trained. Shallower networks with small hidden layer sizes are easier to train but they may not reach the complexity of the problem.

3.3.1.2 Activation Function

Activation function is applied to weighted sum of each layer in order to add non-linearity to the neural networks. There are several choices of activation functions used in neural networks. Some of them are rectified linear unit (ReLU), the hyperbolic tangent (Tanh), and logistic sigmoid (Sigmoid) functions. The formulations for each function can be seen below.

ReLU $$f(x) = \max(0, x)$$ 3.4

Tanh $$f(x) = \tanh(x)$$ 3.5

$$\text{Sigmoid} \quad f(x) = 1/\,(1 + e^{-x}) \qquad 3.6$$

For the regression problem, Tanh and ReLU activation functions are suitable (Pedregosa et al., 2011). Logistic sigmoid function is used in classification problems.

Mathematically, we can represent the relationship between the input data and the output of the network with 3.7, where y is the output of the network, x is the input data, $f^*()$ represents the feedforward propagation algorithm, and θ represents the weights and biases of the network.

$$y = f^*(x, \theta) \qquad 3.7$$

In Figure 3.2 there is a visualization of a simple neural network with 4 input, 3 hidden layers and one output layer. Then, feedforward propagation algorithm equation of this neural network described.

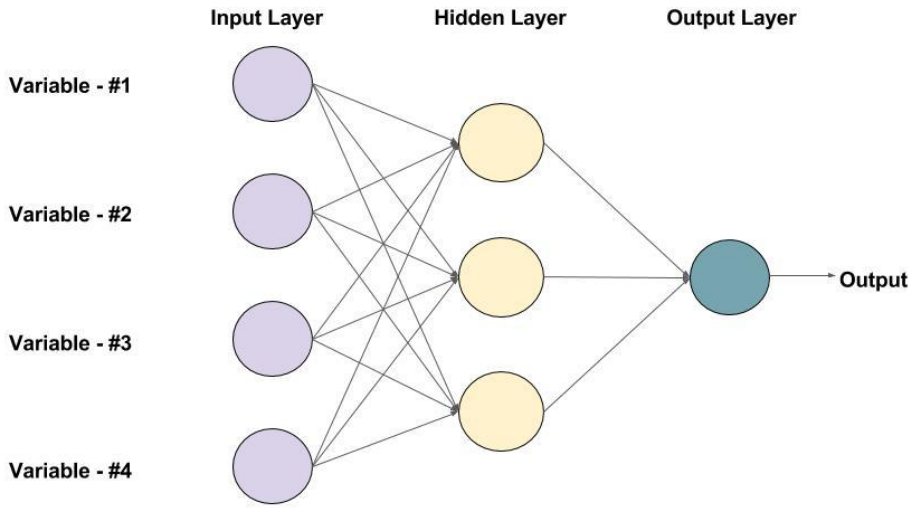


Figure 3.2. An example of a Neural Network with one hidden layer and three nodes

We can show these 4 input layers as $[x_0\, x_1\, x_2\, x_3]$. Then, in order represent hidden layer nodes in each layer, we can use a_i^j where i is activation unit in the node and j

is layer number. Then, weight matrix controlling layer transfer is shown as $\theta^{(j)}$, where j is the layer transformed to $j+1$ layer. These transformations can be linear or non-linear according to neural network aim. This transformation function can be represented with $g()$. After describing the representation, we can show the feedforward algorithm of this simple neural network.

$$a_1^{(2)} = g(\theta_{10}^{(1)} x_0 + \theta_{11}^{(1)} x_1 + \theta_{12}^{(1)} x_2 + \theta_{13}^{(1)} x_3) \quad 3.8$$

$$a_2^{(2)} = g(\theta_{20}^{(1)} x_0 + \theta_{21}^{(1)} x_1 + \theta_{22}^{(1)} x_2 + \theta_{23}^{(1)} x_3) \quad 3.9$$

$$a_3^{(2)} = g(\theta_{30}^{(1)} x_0 + \theta_{31}^{(1)} x_1 + \theta_{32}^{(1)} x_2 + \theta_{33}^{(1)} x_3) \quad 3.10$$

$$f^*(x,\theta) = a_1^{(3)} = g(\theta_{10}^{(2)} a_0^{(2)} + \theta_{11}^{(2)} a_1^{(2)} + \theta_{13}^{(2)} a_2^{(2)} + \theta_{13}^{(2)} a_3^{(2)}) \quad 3.11$$

3.3.2 Backpropagation Algorithm

Feedforward propagation is used to determine output values from input values with the given number of nodes and weights of these nodes. To estimate these weights, neural networks need to be trained. In this process, the backpropagation algorithm is used.

The backpropagation algorithm aims to decrease the error between predicted and exact values. This error is defined as a function with respect to the weight of the nodes of the neural networks. This function is called the loss function or cost function of the neural network.

3.3.2.1 The Loss Function

There are several methods to define a loss function for regression problems. Mean squared error (MSE), root mean square error ($RMSE$), and coefficient of determination (R^2) are the common loss function used in the literature. The formulations of each values are as follows.

$$MSE = \frac{1}{m}\sum_{i=1}^{m}\left(f^*\left(x^{(i)}\right) - y^{(i)}\right)^2 \quad 3.12$$

$$RMSE = \frac{1}{m}\sum_{i=1}^{m}\sqrt{(f^*(x^{(i)}) - y^{(i)})^2} \quad 3.13$$

$$R^2 = 1 - \frac{\frac{1}{m}\sum_{i=1}^{m}\left(f^*\left(x^{(i)}\right) - y^{(i)}\right)^2}{\frac{1}{m}\sum_{i=1}^{m}(f^*(x^{(i)}) - y_{mean})^2} \quad 3.14$$

The loss function is formulated with following equations. The following loss function is mean square error, MSE.

$$f(x,\theta) = \theta_0 + \theta_1 x_1 + \theta_2 x_2 + \theta_3 x_3 \ldots + \theta_n x_n \quad 3.15$$

$$J(\theta_0, \theta_1, \ldots, \theta_n) = \frac{1}{2m}\sum_{i=1}^{m} f^*(x^{(i)}) - y^{(i)})^2 \quad 3.16$$

These formulas written for a regression problem which has n number of features (input parameters), m number of data samples for training. J function is loss function written which respect to node weights, $\theta's$ and y values are the true output values for each data sample.

3.3.2.2 Optimization/Solver Algorithm

After defining the loss function according to true output values and the weights of the neural network, several methods are used to find the optimum point of this error function. Gradient descent algorithm is one of the optimization algorithm selection methods. In this process, arbitrary values are selected for the weights. Then, slopes/gradients with respect to each weight are calculated from the loss function

and these gradients are used to determine new weight values in each iteration. This process continues until acceptable error values are obtained.

The loss or cost function graph of a simple regression problem shown in the Figure 3.3. In addition, figure shows how gradient descent is used to update weights and find optimal weight to minimize the value of cost function.

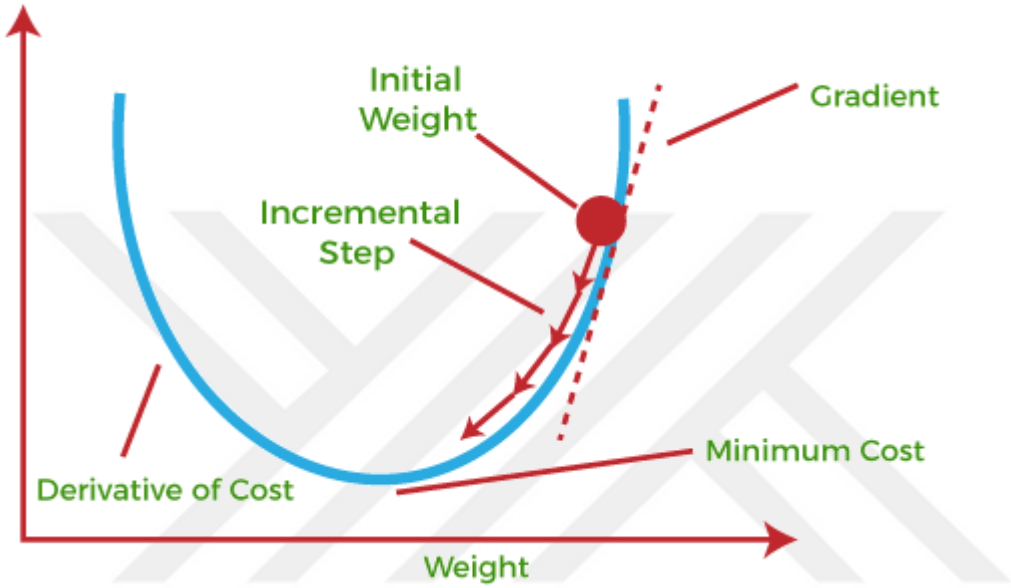


Figure 3.3. Gradient descent algorithm (Pedregosa et al., 2011)

Gradient of the each weight with respect to cost function in 3.16 is calculated in the following equations.

$$\theta_{n,iteration} = \theta_{n,iteration-1} - a\frac{\partial}{\partial\theta_n}J(\theta_0,\theta_1,\ldots,\theta_n) \quad 3.17$$

$$\frac{\partial}{\partial\theta_n}J(\theta_0,\theta_1,\ldots,\theta_n) = \frac{1}{m}\sum_{i=1}^{m}(f^*(x^{(i)}) - y^{(i)}) * x^{(i)} \quad 3.18$$

In this equation a refers learning rate. The learning rate is used to scale gradient descent values to update weight values in each iteration of the training process. Smaller value the learning rate decrease convergence time but lower the step size of the gradient descent of the loss function. This increases the chance of a catching best weight for the minimum loss function value. Bigger values of the learning rate

increase the convergence time but increase also the fluctuation in gradient descent values and the chance of a missing optimum weight values for the minimum loss function. Therefore, learning rate is also very important value to be determined.

In neural networks, computational space is important. In gradient descent all of the data samples are used to calculate loss function since loss functions' derivative values are used to update each weight through iteration. Using all data sample can create computation space problems. Therefore, there are several alternatives of the gradient descent algorithm.

Stochastic Gradient Descent, (SGD) is an alternative version of the gradient descent algorithm. In this process, instead of using of samples for the calculation of loss function, one random sample or a small number of samples used for the calculation of the loss function. This reduces the required computation space.

Another solver algorithm is the Adaptive Moment Estimation (ADAM). This method is also extended version of the SGD. In this method, learning rates are stored for each weight separately and updated for each iteration. This can supply faster and accurate training results.

Another solver algorithm is Limited-memory Broyden-Fletcher-Goldfarb-Shanno algorithm (LBFGS). This algorithm is a quasi-Newton method. In this method, calculated values of loss functions used to create a matrix and these matrices used for the finding optimum weight values of the neural network (Pedregosa et al., 2011).

3.3.3 Hyper parameter selection

Hyperparameters are settings and configurations of the neural network which are not determined with learning. These parameters are determined before learning and they play crucial role in effectiveness of the neural networks. Less convergence time, lower computational space, better performance of prediction results can be achieved with good hyperparameters (Pedregosa et al., 2011).

In this study hyperparameters selection process is done with iterative ways. In this process, models are created for each candidate values for each hyperparameters. Each model train and cross validation scores are saved for comparison. The following hyperparameters must be selected for this study.

- Hidden layer sizes
- Activation function
- Loss function
- Optimization/Solver algorithm selection

In addition to architectural parameters, some generalization parameters must be selected. Generalization capability of a neural network shows how good a neural network model predicts test dataset as well as the train dataset. If the model is complex enough to predict output values for the training dataset, this shows that model has low bias and can replicate complexity of the problem solved with neural network. Model complexity can be increased by the hidden layer size of the model and activation functions selected in each node. More complex model optimizes the training score of the model, but complex models can overfit the train dataset which can lead poor performance on the test data. This situation is called high variance problem and the neural network model results would change if the model trained with different dataset (Hastie et al., 2009).

The Figure 3.4 depicts the idea of bias and variance problems with respect to model complexity. Figure shows that with lower complex model there is bias problems and model cannot perform well on both train and test dataset. Models with high complexity on the other hand, can perform well on train data, but fails in the test data. To overcome this problem there is several methods in the literature.

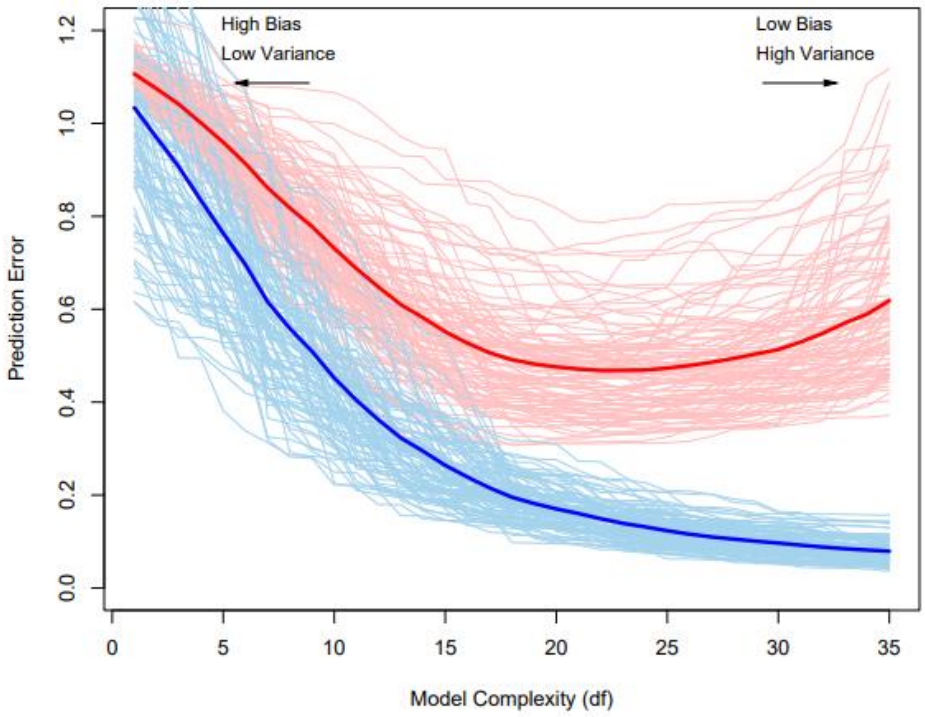


Figure 3.4. Error produced from model with different complexities. Blue curves indicate the training error and red curves indicates the test error (Hastie et al. 2009)

- Regularization

The first method is regularization. In this method, in addition to loss function, the sum of the weight parameters is also tried to be decreased. This method keeps weight values less and make model less sensitive to the training dataset. The updated expression to optimize is given in 3.19.

$$J(\theta_0, \theta_1, \dots, \theta_n) = \frac{1}{2m} \sum_{i=1}^{m} (f^*(x^{(i)}) - y^{(i)}) + \frac{\lambda}{2 * m} * \sum_{j=1}^{n} \theta_n \qquad 3.19$$

The λ value in the equation determines the magnitude of the regularization. Greater values of the lambda make weight values close to the zero and creates a low bias problem since importance of the weight are minimized. The regularization term is chosen in logarithmic scales in literature such as $0.001, 0.01, 0.1$ etc.

- Early stopping

Early stopping involves monitoring the performance of the neural network through iterations and stops the iteration if model stops to improve validation results. This stopping situation can be defined with maximum numbers of iteration value or a threshold error value in the training process.

The Table 3.7 show values that are selected for each hyper parameter value to create a grid search developed for the NN model of this thesis. This selection is combination of the selected hyperparameter values from Demirhan (2022) and Formentin et al. (2017). Each value in this grid will be trained and cross validated. The best values will be selected according to obtained lowest cross validation score.

Table 3.7 Hyperparameters Grid

Hidden layer sizes	*Solver*	*Activation function*	*Loss function*	λ
25, (1 layer)	Adam	Tanh	R^2	0.001
40, (1 layer)	SGD	ReLU	$RMSE$	0.01
50, (1 layer)	L-BFGS			0.04
75, (1 layer)				0.18
100, (1 layer)				0.75
30, 20 (2 layer)				3.16
50, 40 (2 layer)				13.4
85, 50 (2 layer)				56.23

Formentin et al. (2017) states that early stopping doesn't affect the performance of Overtopping-Neural Network tool well. Therefore, early stopping method is not used in this study. Regularization with λ and K-fold cross validation is used to achieve generalization.

The learning rate and maximum number of iteration values is selected as 0.001 and 200 which are Python Sci-kit learn tools default values.

3.3.4 Train, cross validation and test splitting

In order to assess the performance of the neural network and creating the model with proper parameters and architecture, datasets are divided into three categories. These 3 categories are train, cross validation and test. There are no certain division ratios.

Firstly, train and cross validation datasets are used to determine the best model parameters to be selected. These datasets are used in creating the proper neural network model. K-fold is the cross validation method used in this study. In this method train and dataset part of the whole dataset is divided into equally sized batches. Then, one of these batch is used for cross-validation and other remaining batches are used for training purpose. In summary, train phase repeated n times and cross-validated n times with different part of the dataset. Mean scores calculated for each model parameters combination and the best parameters are determined. Formentin et al. (2017) use 50 times training for hyper parameter selection process and this value is adopted also in this study.

Test dataset is created from whole data in the beginning and these data are never used in training process. Therefore, test score is a measure of the generalization capabilities of the model. Test dataset values predicted with the model created with training dataset are compared with measured test dataset values. This comparison also repeated 50 times and the final test score is the mean test scores of 50 test scores.

In this study, test data extracted from four datasets and remained data used for training and cross validation. Test portions for each dataset show in the Table 3.8.

Table 3.8 Test portions for each dataset

Dataset	*Test Size (%)*	*Count*
EU_VER	20	346
METU_VER	20	26
METU_SWB	20	41
LABIMA_SWB	50	22

LABIMA_SWB dataset is aimed to be main test experiments for the evaluation of the model. Therefore, test size is higher for LABIMA_SWB dataset. The remaining 1674 data used in training and cross validation processes. 80 percent of this data used for training and 20 percent used in cross validation.

When calculating cross-validation and test scores, $RMSE$ and R^2 methods are used.

3.4 Model Evaluation

After selection of the hyper parameters, the final model must be evaluated. In this study, the final model assessed by 4 methods. These methods are learning curves, accuracy metrics, literature empirical formulas, and domain validity check. These checks are used to measure performance of the model and whether the model can be further improved.

3.4.1 Learning curves

The learning curves are used to measure the model scalability. In this method, many models are created with datasets which has different number of data samples. Then, train and test scores of each model are compared with sample size of the dataset. This gives us a scale of how the model performance increase if we find more data samples for the model.

3.4.2 Domain Validity Check

The predicted values by neural networks are plotted against the measured values of the training dataset. This plot helps users check whether the prediction values are within the training dataset. This gives us a measure of the reliability of the neural network predictions (Formentin et al. (2017).

3.4.3 Accuracy metrics

The final selected model architecture is compared with test datasets extracted at the beginning from the whole dataset. Predicted wave overtopping values are compared with measured wave overtopping values. In addition, the prediction error percentage is compared with crest elevations, R_c which is considered the main overtopping parameter (Formentin et al. (2017).

3.4.4 Literature Empirical Formulas

In order to measure performance of the created wave overtopping model, prediction results are compared with several empirical formulas in the literature. Literature formulas of vertical walls with SWB and superstructures are discussed in the section 2.1. These formula results are compared with prediction with NN respect to R_c/H_{m0}.

3.5 Software Used

Sci-kit sklearn library of the Python programming language is used for creation of the Neural Network tools. This tool provides training, cross validation functionalities and hyper parameters selection algorithms.

In order to create neural network with this tool Multi-Layer Perception class is used. This class can be initiate with the architectural and hyper-parameters mentioned in the sections 3.3.1, 3.3.2, and 3.3.3 and its fit and predict methods can be used for training of the neural network calculating the output.

The performance of the Sci-kit sklearn library is very good. In this study, all prediction values are calculated as mean of the 50 prediction values for each input sample. A test dataset which has around 300 input samples estimated approximately in 3 seconds. In training, for each hyper-parameter combination of hyper parameters the model trained 50 times. 480 hyper-parameter combinations are tried and this makes 19200 train process for model. This train process is done in 3 hours.

Scaling and transformation of the data mentioned in 3.1 and 3.2 are done with Pandas and Numpy libraries of the Python.

CHAPTER 4

RESULTS and DISCUSSION

In this chapter, results of the model creation and evaluation parts are presented. Firstly, model architecture of the new created neural network model is selected. The scalability of the model is evaluated with learning curves. Then, training performance of the neural network is depicted with domain validity scatter graphs. Finally, performance of the new neural network is evaluated against empirical formulas in the literature and the existing Eurotop Neural Network tool.

4.1 Grid Search Results

Hyper-parameters and ANN architecture values listed in Table 3.7 are trained and cross validated. Model trained according all of the 480 hyper-parameter combinations. Following results are the best 7 score hyper-parameter values. Metrics are mean values of the test results of 50 train results. The results of all the combinations are presented in Appendix.

Table 4.1 Best results for the vertical wall ANN

Solver	*Activation Function*	*Alpha*	*Hidden Layer Size*	*RMSE*	R^2
L-BFGS	ReLU	0.18	(85, 50)	0.886123	0.002396
ADAM	ReLU	0.18	(85, 50)	0.840861	0.003515
ADAM	ReLU	0.18	(50, 40)	0.835575	0.003535
L-BFGS	ReLU	0.18	(30, 20)	0.835131	0.002671
L-BFGS	ReLU	0.75	(30, 20)	0.813851	0.003682
L-BFGS	ReLU	0.75	(50,)	0.808435	0.003567

According to Table 4.1 L-BFGS solver and ReLU activation function gave best results. After selection of this L-BFGS and ReLU as solver and activation function hyper-parameters, in order to select hidden layer sizes and alpha values following figure is provided. In Figure 4.1, test results for different hidden layer sizes and alpha hyper-parameter candidates shown in section 3.3.3 is depicted by R^2.

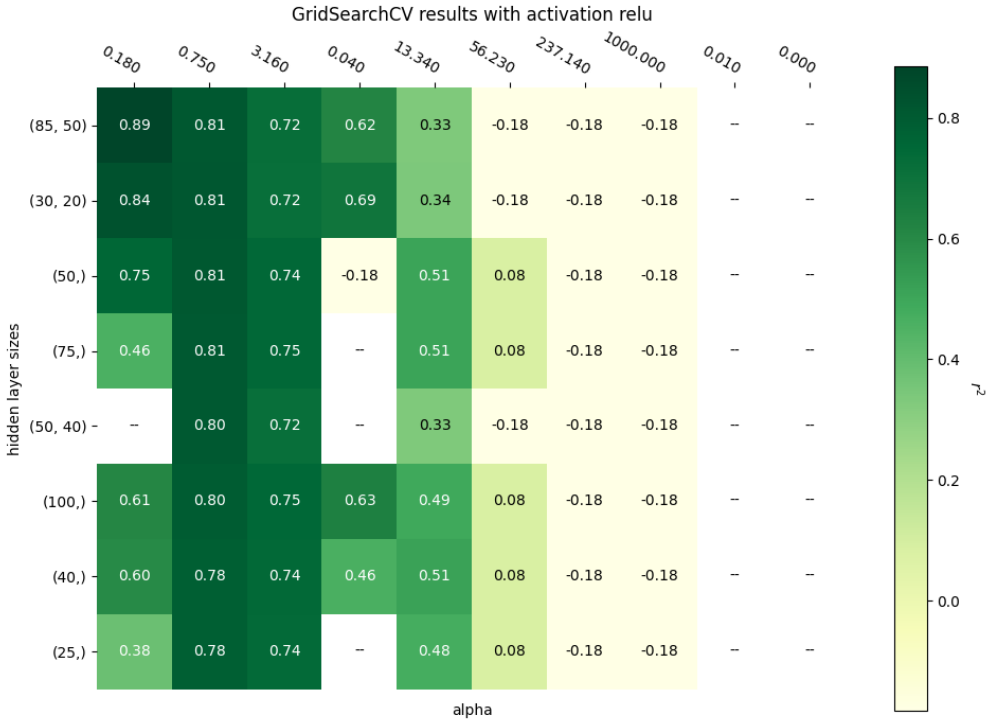


Figure 4.1. R^2 heat map of hidden layer sizes and alpha hyper-parameters candidates

From Figure 4.1, hidden layer sizes and alpha value are selected as $(85,\ 50)$ and 0.18. The final model hyper parameters are as follows.

Table 4.2 Selected Hyper-parameters

Parameter	*Value*
Alpha	0.18
Hidden Layer Size	(80, 50)
Solver	L-FBGS
Activation Function	ReLU

4.2 Learning Curves

After selection of the hyper-parameters, model trained with different train dataset with different sample sizes. As can be seen in the Figure 4.2, models cross validation scores become closer for greater samples sizes. This tells that our model performance increase when we train the model with more data. Although, difference between training and cross validation scores are not very high, getting more data gives better performance on estimation of wave overtopping values. This shows that when more data become available in the literature, the model can be further improved.

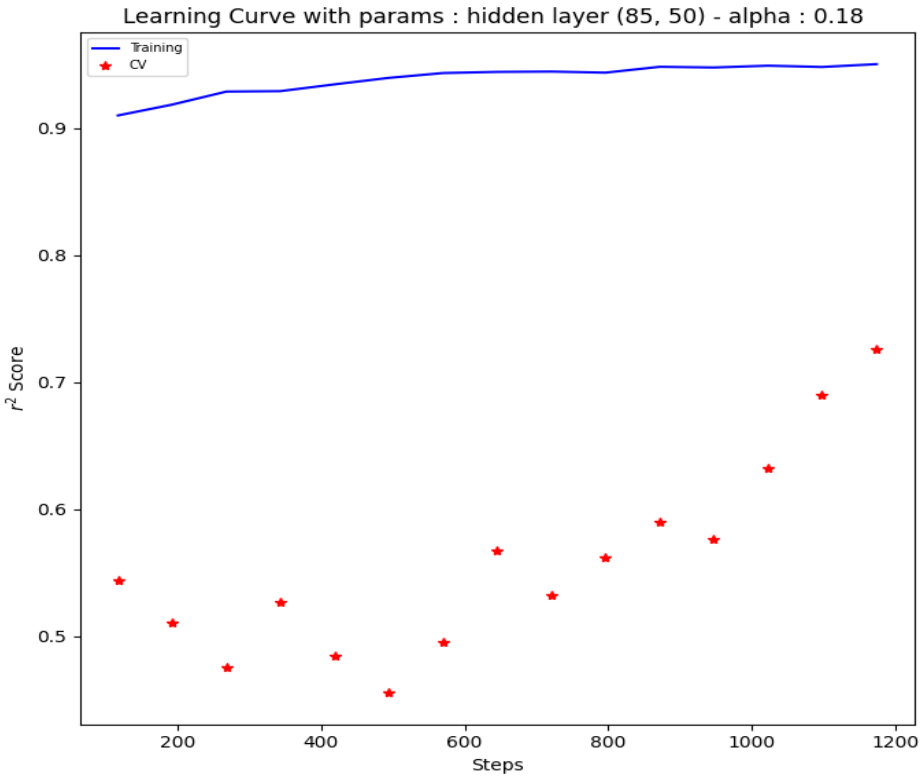


Figure 4.2. Learning curve of selected vertical wall ANN tool

4.3 Domain Validity of the New Neural Network

After selection of the neural network architecture, this model can be used to predict to wave overtopping values other than that training data. The Figure 4.3 contains

both training wave overtopping values and the predicted wave overtopping values of the test experiment datasets which excluded from the training process of the neural network.

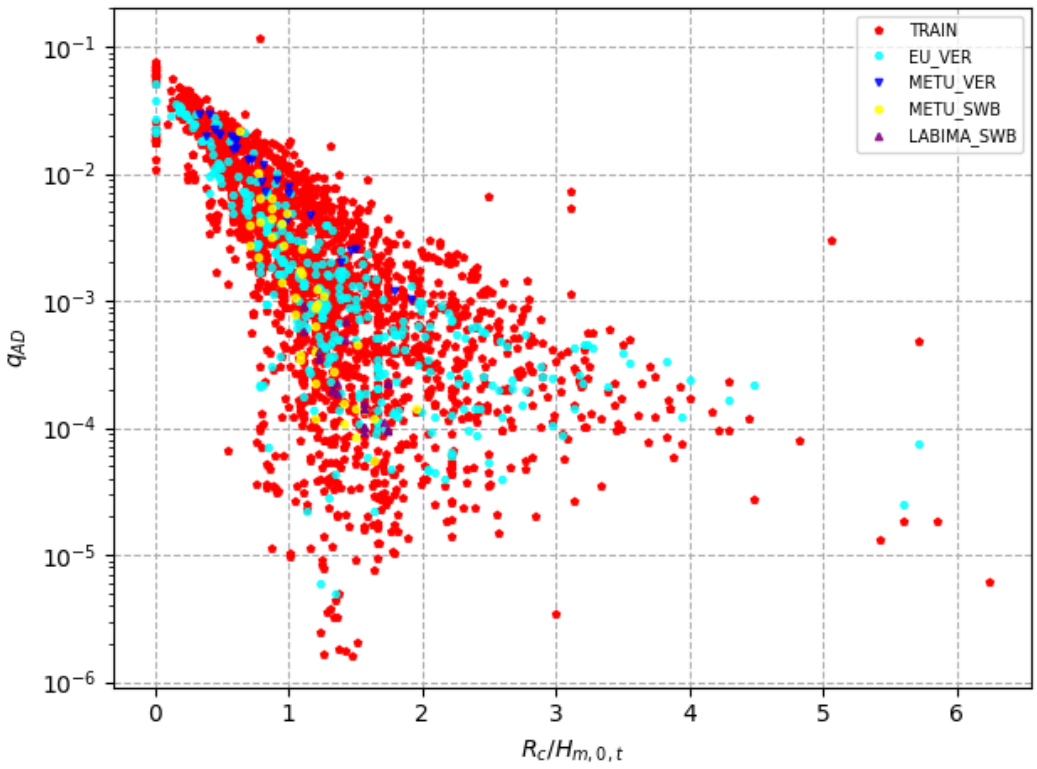


Figure 4.3. Training measured and test prediction wave overtopping values scatter plot

According to figure Figure 4.3, test wave overtopping prediction of the METU_NN model doesn't exceed the training wave overtopping values which shown as red dots in the figure. Only in relative freeboard values greater than 5, there is few data for training. Some of the EU_VER test dataset predictions are in this range but not exceed training data domain also.

4.4 Accuracy metrics

METU_NN model evaluated against literature empiric formulas which will be called as EMPIRIC, and existing Eurotop wave overtopping ANN tool which will be called as EU_NN in the following sections.

EU_NN is not capable of predicting wave overtopping values at vertical wall with SWB and its superstructures. Therefore, METU_VER and EU_VER datasets are used to compare EU_NN and METU_NN models only. Table 4.3 show R^2 and $RMSE$ values of each prediction methods.

Table 4.3 Accuracy of the predictions according to models

Model	*EU_VER*		*METU_VER*		*METU_SWB*		*LABIMA_SWB*	
	R^2	*RMSE*	R^2	*RMSE*	R^2	*RMSE*	R^2	*RMSE*
EU_NN	0.42	0.01015	0.91	0.00927	-	-	-	-
METU_NN	0.92	0.00287	0.97	0.00375	0.96	0.00077	0.78	0.00012
EMPIRIC	0.80	0.00505	0.97	0.00446	0.98	0.00053	0.84	0.00067
q_{AD_mean}	0.00531		0.01597		0.00253		0.00033	

According to Table 4.3, EU_NN showed the worst performance on both EU_VER and METU_VER datasets. EU_NN model has R^2 values around 0.42 which shows that this model can't express variation in the data well. Although, EU_NN model doesn't perform well on EU_VER dataset, the model has good R^2 value of 0.91 for METU_VER . EU_VER datasets consists of many experiment results from the literature. The data cleaning of this thesis presented in section 3.1.4. The performance difference in EU_VER and METU_VER datasets can be explained by data variability of the EU_VER dataset. Data cleaning process may be improved or the datasets can shrink to specified experiment setups only. In addition, EU_NN model has higher values of $RMSE$ in both EU_VER and METU_VER datasets. The other two model have $RMSE$ values half of the EU_NN model.

If we compare METU_NN and EMPIRIC, EMPIRIC predictions are more accurate and can represent variations of the data in METU_SWB dataset. Since, EMPIRIC prediction formulas used in this thesis generated from METU experiment setup this over performing can be acceptable. METU_NN metric values are not much different from EMPIRIC predictions. However, in LABIMA_SWB datasets METU_NN model has lower $RMSE$ values than EMPIRIC formulas. As discussed in section 2.2.4, EMPIRIC formula of Kisacik, Ozyurt Tarakcioglu and Cappietti (2022) created this formula for 3 different setup type of CC5, CC6 and CC8. In this thesis all types used in the tests and training phases. METU_NN used all 5 type in training dataset. Therefore, METU_NN over performing can be reasonable.

In order to observe performance in detail measured and predicted non-dimensinoal wave overtopping values are plotted. In addition, since relative freeboard $R_c/H_{m0,t}$ is main parameter for wave overtopping value, relative freeboard versus error ratio is plotted for each test datasets. 4.1 used in error percentage.

$$q_{AD,error} = \left(q_{AD,predicted} \,/\, q_{AD,measured}\right) \qquad 4.1$$

4.4.1 EU_VER Test Dataset

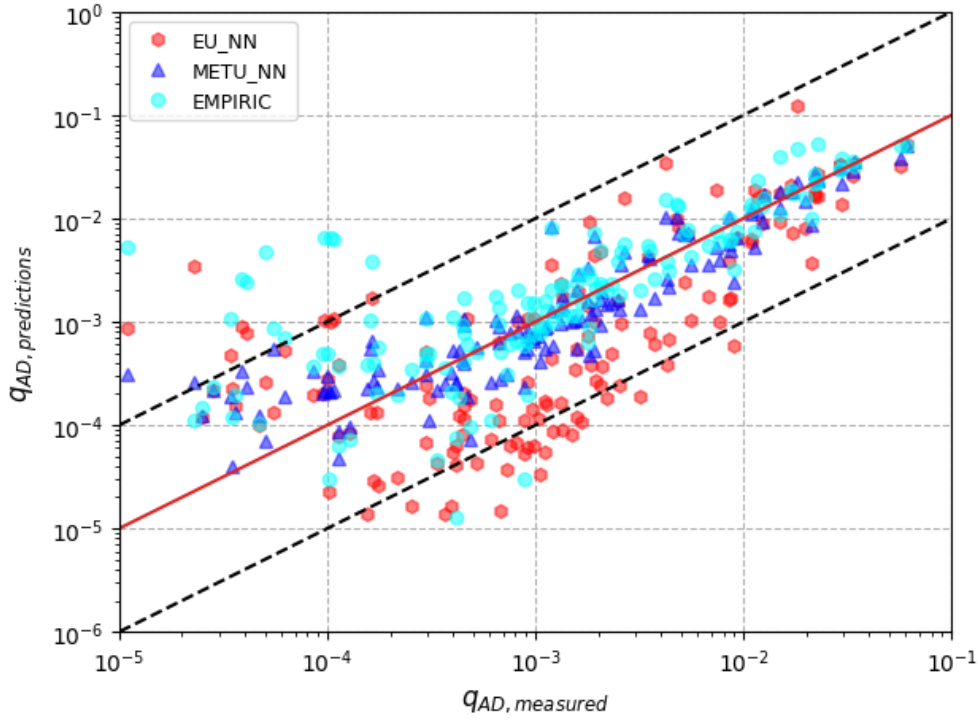


Figure 4.4. EU_VER dataset non-dimensional wave overtopping values (solid line: prediction equal to measured rate, dashed lines: prediction equal to 10 times higher and lower than the measured rate)

In Figure 4.4, scatter graphs of the METU_VER datasets represented. Both three model overestimate wave overtopping at lower wave overtopping values. Although METU_NN makes better estimations than EMPIRIC and EU_NN on non-dimensional wave overtopping values lower than 10^{-4}, estimations exceeds 10 times higher values limit which shown by dashed lines. METU_NN and EMPIRIC make good estimations on non-dimensional wave overtopping values greater than 10^{-4}. EU_NN underestimates wave overtopping in this range.

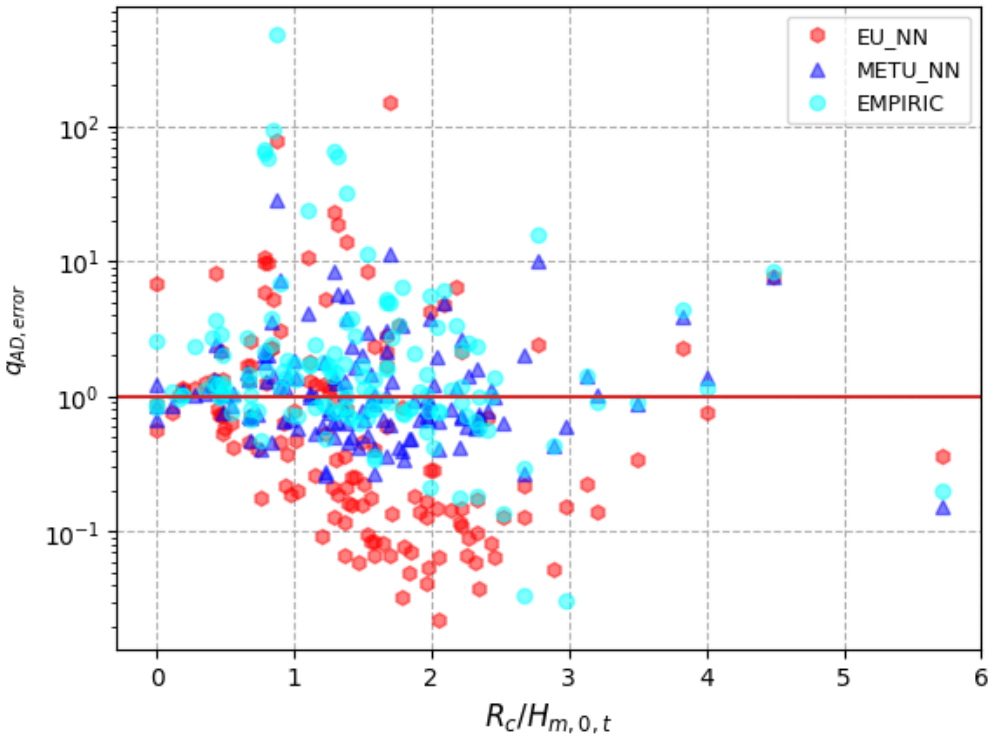


Figure 4.5. EU_VER dataset prediction error ratios of non-dimensional wave overtopping values

According to Figure 4.5 significant underestimation clearly seen for EU_NN especially for range of $1 < R_c/H_{m,0,t} < 3$. The errors are more balanced for the other two prediction methods. There is no clear distinction in the error range for relative freeboard. Although range around 1, shows slightly higher errors for the other two methods.

4.4.2 METU_VER Test Dataset

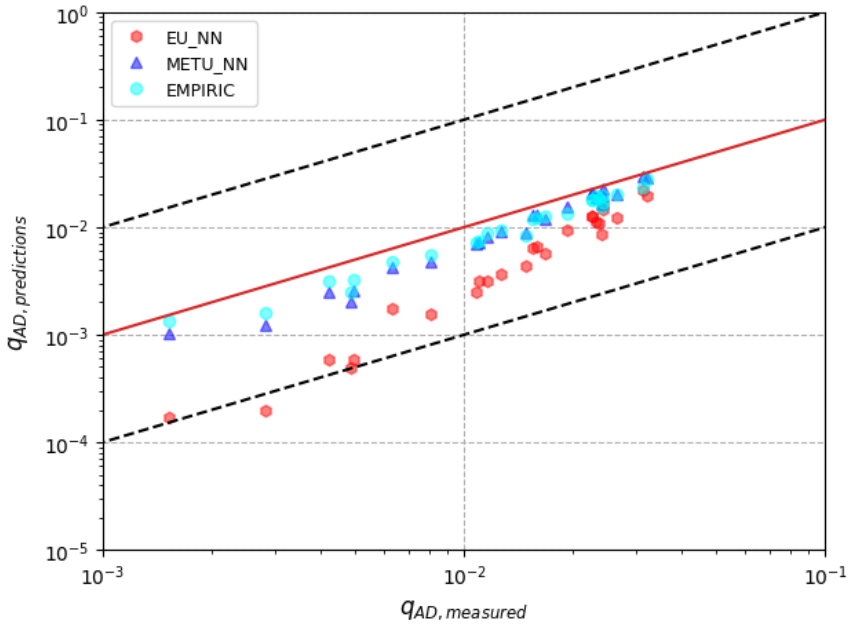


Figure 4.6. METU_VER dataset non-dimensional wave overtopping values (solid line: prediction equal to measured rate, dashed lines: prediction equal to 10 times higher and lower than the measured rate)

In Figure 4.6, scatter graphs of the METU_VER datasets represented. As we can see from the figure both METU_NN and EMPIRIC models shows very good fit for the wave overtopping values. EMPIRIC model performed slightly better on all ranges of non-dimensional wave overtopping values. EU_NN model generally underestimates the wave overtopping values and difference in higher than the other models. This underestimation increases in lower wave overtopping values. Almost all models' predictions fall into range of 10 times higher and 10 times lower non-dimensional wave overtopping values and this resembles with the results shown in the Table 4.3.

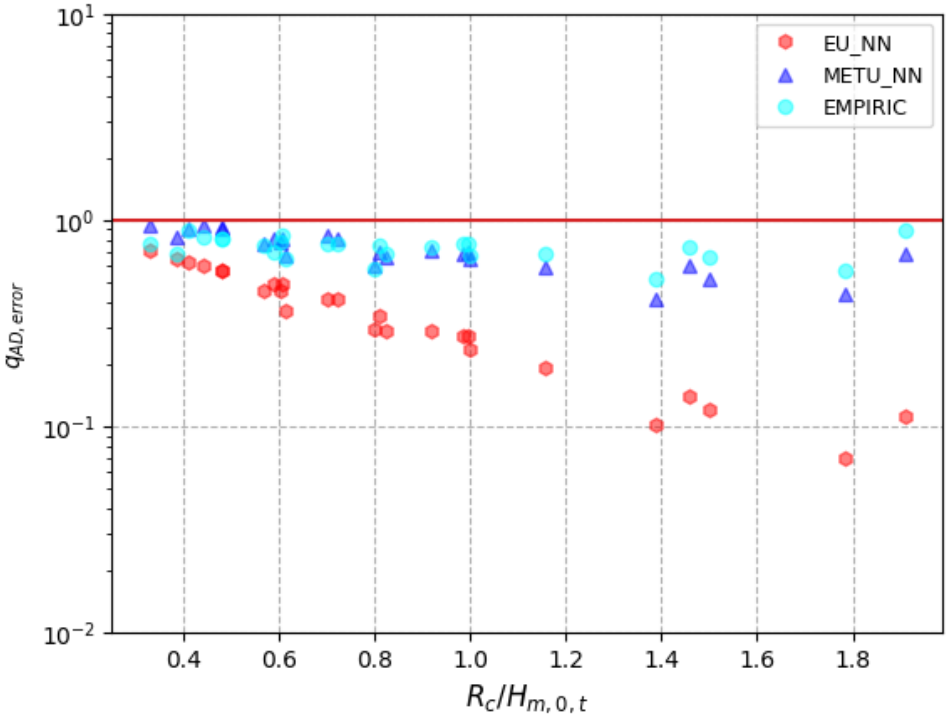


Figure 4.7. METU_VER prediction error ratios of non-dimensional wave overtopping values

According to Figure 4.7 error ratios in all prediction methods are higher in higher relative freeboard values which can be expected since in higher relative freeboard values there are less wave overtopping values. Lower wave overtopping values show more uncertainty and higher error ratios can be observed (Zanuttigh et al., 2017). While there is a clear relationship between error and relative freeboard for EU_NN, the error stabilizes for the other two methods for higher freeboard values.

4.4.3 METU_SWB Test Dataset

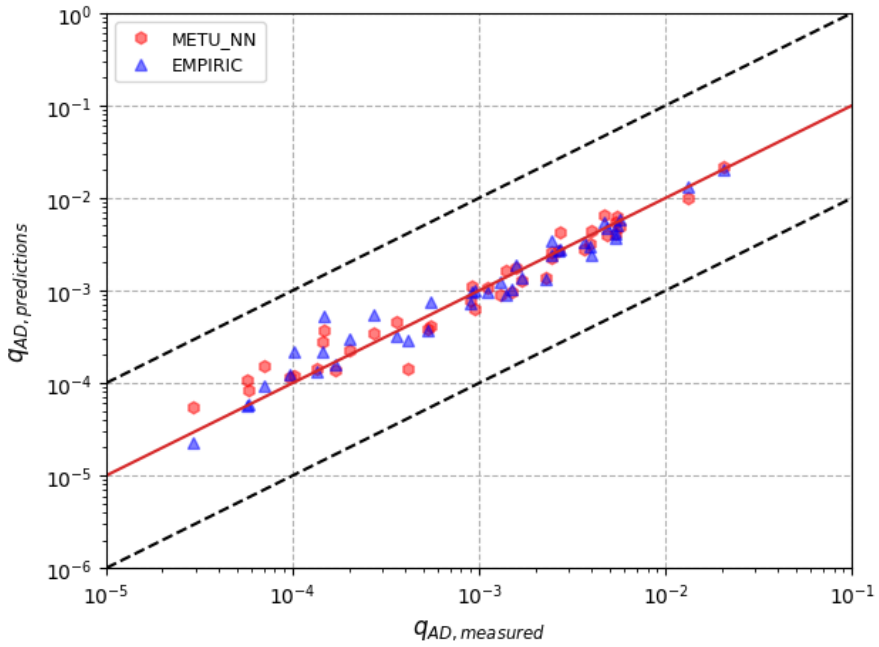


Figure 4.8. METU_SWB dataset non-dimensional wave overtopping values (solid line: prediction equal to measured rate, dashed lines: prediction equal to 10 times higher and lower than the measured rate)

In Figure 4.8, scatter graphs of the METU_SWB datasets represented. As we can see from the figure both prediction method shows very good fit for the wave overtopping values. All values are in the range of 10 times bigger or lower non-dimensional wave overtopping values. Although, the fit on the measured wave overtopping values are good, fit becomes worse on measured values lower than 10^{-3}. This uncertainty increase is expected at lower wave overtopping values (Zanuttigh et al., 2017).

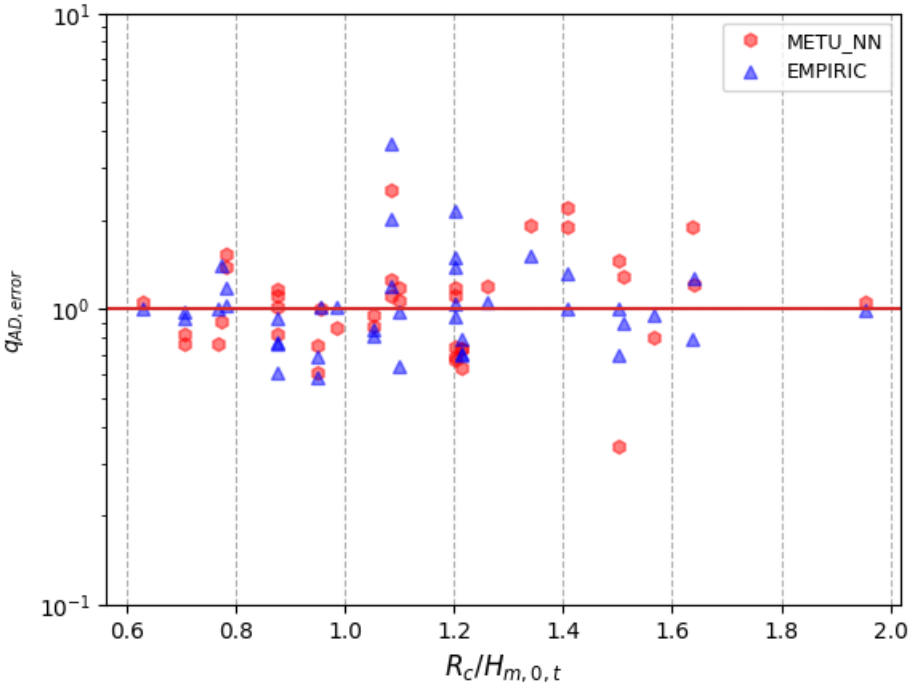


Figure 4.9. METU_SWB prediction error ratios of non-dimensional wave overtopping values

According to Figure 4.9, error ratios in both prediction models show good prediction performance. Error ratios are higher in 1 to 1.6 relative freeboard values but in acceptable amounts.

4.4.4 LABIMA_SWB Test Dataset

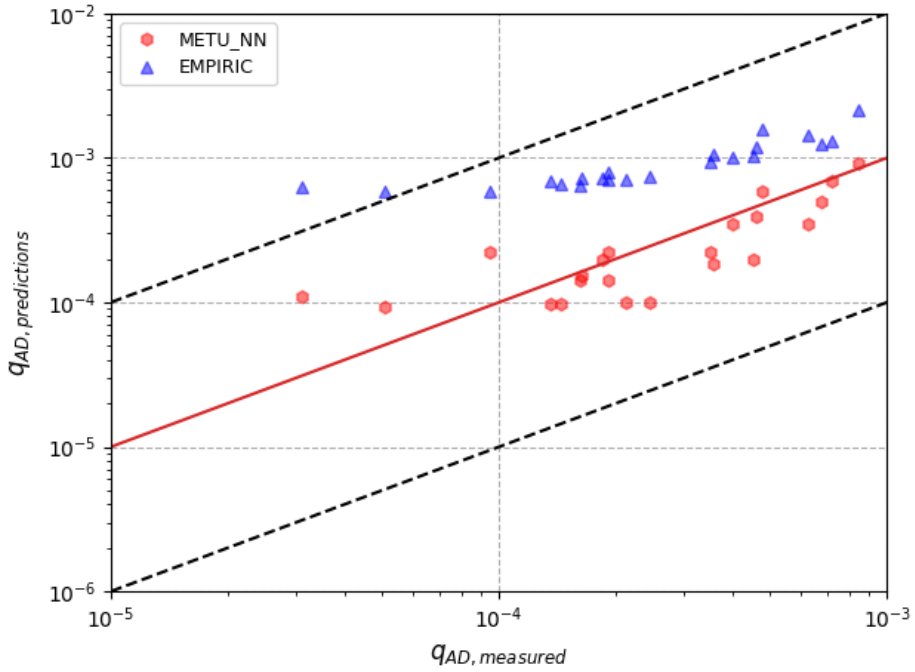


Figure 4.10. LABIMA_SWB dataset non-dimensional wave overtopping values (solid line: prediction equal to measured rate, dashed lines: prediction equal to 10 times higher and lower than the measured rate)

In Figure 4.10, scatter graphs of the LABIMA_SWB test dataset is represented. Both models overestimate wave overtopping values at non dimensional wave overtopping values lower than 10^{-4}. In this range METU_NN has better estimation values. At non dimensional wave overtopping values greater than 10^{-4}, values become more closer to the measured values but, EMPIRIC model overestimates and METU_NN model underestimates the wave overtopping values. The METU_NN again has less difference with actual values. $RMSE$ values were lower in METU_NN model which shown in the Table 4.3. This plot also shows that METU_NN have more accurate values.

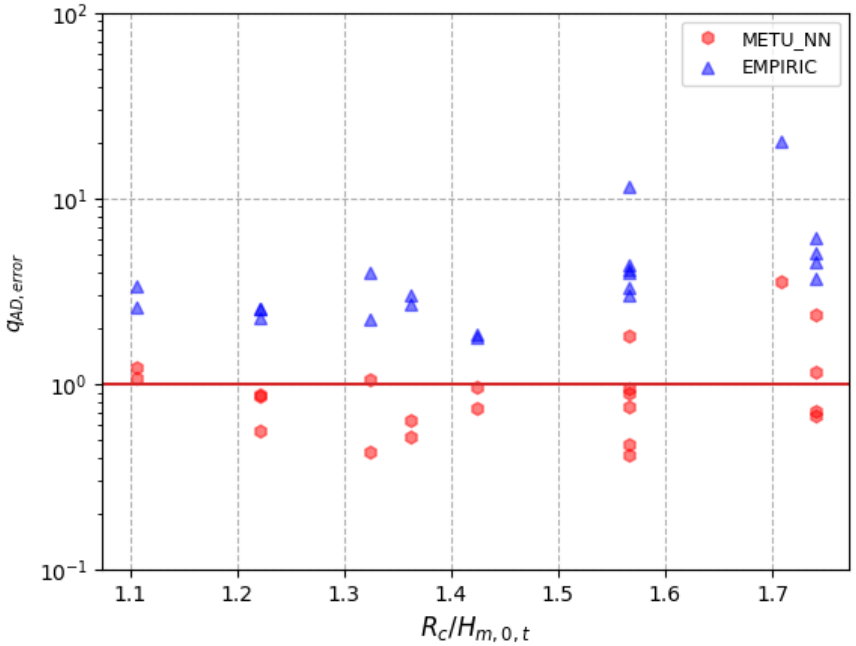


Figure 4.11. LABIMA_SWB ratios error percentage of non-dimensional wave overtopping values

According to Figure 4.11 error ratios in both prediction methods are higher in higher freeboard values. This graph also show that there are other parameters that need to be considered to increase accuracy of the models in addition to $R_c/H_{m,0,t}$.

CHAPTER 5

CONCLUSIONS

As the main motivation of this thesis, the METU_NN artificial neural network model is created. This model can calculate wave overtopping values on vertical walls with SWB and its superstructures.

A database consists of 2116 physical tests created to train and test the METU_NN model. The hydraulic and structural schematization of the database contains vertical walls, SWBs, and the other SWB superstructures geometries.

17 non dimensional input parameter were selected for the model and these values can represent any vertical walls with SWB and its superstructures geometries and model can predict wave overtopping values on these structures.

The architecture of the METU_NN model was optimized by training and cross-validating the METU_NN model for 480 different hyper-parameter with combination 50 different folds obtained from the study database.

METU_NN model is evaluated against test dataset which that was not included in training process. In addition, METU_NN predictions compared with existing literature formulas and The Overtopping-Neural Network of EurOtop (2018).

The following results are observed after the studies mentioned above.

- Optimized METU_NN model present good performance on training data with 0.33 RMSE value of q^* calculated with Equation 3.3 (values between 0-1).
- METU_NN model performed better than The Overtopping-Neural Network on plain vertical wall test datasets (EU_VER, METU_VER)
- METU_NN performed better than existing empirical formulas on literature on plain vertical wall test datasets (EU_VER, METU_VER). In addition,

METU_NN performed as good as empiric formulas on vertical walls with SWB and its superstructures test datasets (METU_SWB, LABIMA_SWB)

All accuracy metrics presented in Section 4.4 and above concluded results are studied from experimental results. Therefore, when using this tool, it must be considered that this tool was developed from data with no wind effects and under lab conditions using fresh water. In addition, database ranges given in Section Table 3.4 have to be checked when making estimation on wave overtopping discharges in order to prevent the use of the model out of its training fields.

After concluding the findings of the thesis, there are several issues that can be stated as further studies.

- In this thesis, vertical walls with SWB and its superstructures datasets are limited to data from only 2 physical experiments. In order to increase and generalize the performance of the METU-NN model on these structures, more test experiments with vertical walls with SWB and its superstructures can be included in the training database.
- Impulsiveness of wave conditions is an important criteria on wave overtopping discharges. In this study, impulsiveness of wave conditions wasn't included directly in the model optimization processes. Impulsiveness of the wave conditions can be included as an input parameter and effects of the impulsive wave conditions can be examined.
- In vertical walls with SWB structures the promenade section of the structure can be filled with water and in long periods this can create an increase on the successive wave overtopping discharge values. In this study, this process is not taken into account. A relation between storm duration or volume in SWB and wave overtopping discharge value can be investigated.
- Numerical models are another method for the calculation of the wave overtopping in sea defense structures. METU_NN can be evaluated against also numerical models.

REFERENCES

Crema, I., Cappietti, L., & Aminti, P.I.E.R. (2009). Laboratory measurements of wave overtopping at plain vertical wall breakwaters in presence of an overspill stilling basin. In IAHR-4th International Short Conference/Course on Applied Coastal Resarch (pp. 353-360). Nuova Editoriale Bios.

De Rouck, J., Verhaeghe, H., & Geeraerts, J. (2009). Crest level assessment of coastal structures—General overview. Coastal Engineering, 56(2), 99-107.

Di Risio, M., Beltrami, G. M., & De Girolamo, P. (2007). Laboratory investigation on wave overtopping of composite breakwaters: The port of Civitavecchia case. In Coastal Engineering 2006: (In 5 Volumes) (pp. 4616-4627).

EurOtop, 2018. Manual on Wave Overtopping of Sea Defenses and Related Structures, an Overtopping Manual Largely Based on European Research, but for Worldwide Application, second ed. 2018. http://www.overtopping-manual.com/

Formentin, S. M., Zanuttigh, B., & van der Meer, J. W. (2017). A neural network tool for predicting wave reflection, overtopping and transmission. Coastal Engineering Journal, 59(1), 1750006-1.

Formentin, S. M., & Zanuttigh, B. (2018). A methodological approach for the development and verification of artificial neural networks based on an application to wave–structure interaction processes. Coastal Engineering Journal, 60(3), 260-279.

Franco, L., De Gerloni, M., & Van der Meer, J. W. (1995). Wave overtopping on vertical and composite breakwaters. In Coastal Engineering 1994 (pp. 1030-1045).

Hastie, T. (2009). et. all. Statistics The Elements of Statistical Learning. Springer Ser Stat, 27, 745.

Goda, Y. (2010). Random seas and design of maritime structures (Vol. 33). World Scientific Publishing Company.

Kisacik, D., Tarakcioglu, G. O., & Baykal, C. (2019). Stilling wave basins for overtopping reduction at an urban vertical seawall–The Kordon seawall at Izmir. Ocean Engineering, 185, 82-99.

Kisacik, D., Tarakcioglu, G. O., & Cappietti, L. (2022). Adaptation measures for seawalls to withstand sea-level rise. Ocean Engineering, 250, 110958.

Shalev-Shwartz, S., & Ben-David, S. (2014). Understanding machine learning: From theory to algorithms. Cambridge university press.

Tuan, T. Q. (2013). Influence of low sea-dike crown-walls on wave overtopping discharge. Coastal Engineering Journal, 55(4), 1350013-1.

van der Meer, J., & Bruce, T. (2014). New physical insights and design formulas on wave overtopping at sloping and vertical structures. Journal of Waterway, Port, Coastal, and Ocean Engineering, 140(6), 04014025.

Van Doorslaer, K., De Rouck, J., Boderé, T.O.B.I.A.S., Vanhouwe, G., & Troch, P. (2010). The influence of a berm and a vertical wall above SWL on the reduction of wave overtopping. Proc. Coastlab, 2010, 10.

Van Doorslaer, K., De Rouck, J., Audenaert, S., & Duquet, V. (2015). Crest modifications to reduce wave overtopping of non-breaking waves over a smooth dike slope. Coastal Engineering, 101, 69-88.

van Gent, M. R., van den Boogaard, H. F., Pozueta, B., & Medina, J. R. (2007). Neural network modelling of wave overtopping at coastal structures. Coastal engineering, 54(8), 586-593.

Verhaeghe, H., De Rouck, J., & van der Meer, J. (2008). Combined classifier–quantifier model: a 2-phases neural model for prediction of wave overtopping at coastal structures. Coastal Engineering, 55(5), 357-374.

Zanuttigh, B., Formentin, S. M., & Van der Meer, J. W. (2014). Advances in modelling wave-structure interaction through artificial neural networks. Coastal Engineering Proceedings, 1(34), 69.

Zanuttigh, B., Formentin, S. M., & van der Meer, J. W. (2016). Prediction of extreme and tolerable wave overtopping discharges through an advanced neural network. Ocean Engineering, 127, 7-22.

Zanuttigh, B., & Formentin, S. M. (2018). Reduction of the wave overtopping discharge at dikes in presence of crown walls with bullnoses. In Proceedings of 36th International Conference on Coastal Engineering (ICCE) (pp. 1-14). ASCE.

Zerbini, S., Raicich, F., Prati, C. M., Bruni, S., Del Conte, S., Errico, M., & Santi, E. (2017). Sea-level change in the Northern Mediterranean Sea from long-period tide gauge time series. Earth-Science Reviews, 167, 72-87.

APPENDICES

A. Grid Search Results for each Hyper-parameter Combination

Table A.1 Grid search results

Rank	*Activation Function*	*Alpha*	*Hidden Layer Size*	*Solver*	R^2	*RMSE*
1	relu	0.18	(85, 50)	lbfgs	0.886123	0.002396
2	relu	0.18	(85, 50)	adam	0.840861	0.003515
3	relu	0.18	(50, 40)	adam	0.835575	0.003535
4	relu	0.18	(30, 20)	lbfgs	0.835131	0.002671
5	relu	0.75	(30, 20)	lbfgs	0.813851	0.003682
6	relu	0.75	(50,)	lbfgs	0.808435	0.003567
7	relu	0.75	(85, 50)	lbfgs	0.80684	0.003575
8	relu	0.75	(75,)	lbfgs	0.805083	0.003497
9	relu	0.75	(100,)	adam	0.805077	0.003986
10	relu	0.75	(50, 40)	lbfgs	0.803799	0.003604
11	tanh	0.18	(50, 40)	adam	0.798633	0.004181
12	relu	0.75	(100,)	lbfgs	0.796866	0.00354
13	relu	0.75	(40,)	lbfgs	0.782885	0.003716
14	relu	0.75	(25,)	lbfgs	0.781875	0.003775
15	tanh	0.04	(85, 50)	adam	0.766903	0.004413

16	tanh	0.75	(50, 40)	lbfgs	0.758224	0.004265
17	relu	0.18	(50,)	lbfgs	0.754526	0.002847
18	relu	3.16	(100,)	lbfgs	0.751117	0.004695
19	tanh	0	(85, 50)	adam	0.749461	0.004527
20	tanh	0.01	(85, 50)	adam	0.749258	0.00457
21	relu	3.16	(75,)	lbfgs	0.747184	0.00472
22	tanh	0.75	(50,)	lbfgs	0.744997	0.004219
23	relu	3.16	(50,)	lbfgs	0.744847	0.004741
24	tanh	0.18	(85, 50)	adam	0.744113	0.004813
25	tanh	0.75	(30, 20)	lbfgs	0.744085	0.004411
26	relu	0.18	(30, 20)	adam	0.743355	0.004587
27	tanh	0.75	(40,)	lbfgs	0.742962	0.004287
28	tanh	0.75	(85, 50)	lbfgs	0.74254	0.004333
29	relu	3.16	(40,)	lbfgs	0.74158	0.004779
30	relu	3.16	(25,)	lbfgs	0.736756	0.004771
31	relu	0.75	(75,)	adam	0.725909	0.004738
32	tanh	0.75	(100,)	lbfgs	0.721718	0.004468
33	relu	3.16	(85, 50)	lbfgs	0.71962	0.005011
34	tanh	0.75	(25,)	lbfgs	0.719602	0.004508
35	relu	3.16	(30, 20)	lbfgs	0.716835	0.005057
36	relu	3.16	(50, 40)	lbfgs	0.71527	0.005044
37	relu	3.16	(100,)	sgd	0.70948	0.005124

38	tanh	0.04	(50, 40)	adam	0.707984	0.004842
39	tanh	0.75	(75,)	lbfgs	0.704998	0.004482
40	relu	0.75	(50, 40)	adam	0.700995	0.005205
41	tanh	3.16	(25,)	lbfgs	0.700712	0.005245
42	tanh	0.18	(40,)	lbfgs	0.699498	0.00348
43	relu	0.75	(30, 20)	adam	0.693723	0.005204
44	tanh	0.01	(50, 40)	adam	0.693472	0.004961
45	relu	0.04	(50, 40)	adam	0.690383	0.004542
46	relu	0.04	(30, 20)	lbfgs	0.689159	0.00242
47	tanh	0	(50, 40)	adam	0.688025	0.005005
48	tanh	3.16	(40,)	lbfgs	0.686499	0.005418
49	tanh	3.16	(100,)	lbfgs	0.680804	0.005458
50	tanh	0.18	(30, 20)	lbfgs	0.675957	0.003535
51	relu	3.16	(50,)	sgd	0.667303	0.005463
52	tanh	0.75	(25,)	adam	0.666498	0.005455
53	tanh	0.18	(25,)	lbfgs	0.666232	0.0039
54	tanh	3.16	(85, 50)	lbfgs	0.665501	0.005608
55	relu	0.01	(50, 40)	adam	0.662705	0.004803
56	tanh	3.16	(50,)	lbfgs	0.66246	0.005477
57	tanh	0	(40,)	sgd	0.662398	0.00553
58	tanh	0.01	(40,)	sgd	0.662347	0.005531
59	tanh	0.04	(40,)	sgd	0.662207	0.005533

60	tanh	0.18	(40,)	sgd	0.661594	0.00554
61	tanh	3.16	(30, 20)	lbfgs	0.661375	0.00564
62	tanh	0.75	(40,)	sgd	0.660445	0.005574
63	tanh	3.16	(50, 40)	lbfgs	0.660212	0.005648
64	relu	0	(50, 40)	adam	0.658804	0.00484
65	relu	0.04	(85, 50)	adam	0.657732	0.004512
66	relu	0.75	(85, 50)	adam	0.654847	0.005599
67	tanh	0.18	(85, 50)	lbfgs	0.648971	0.003689
68	tanh	3.16	(75,)	lbfgs	0.642325	0.00554
69	relu	0.04	(100,)	lbfgs	0.634557	0.002385
70	tanh	0.18	(30, 20)	adam	0.628392	0.00568
71	tanh	0.75	(40,)	adam	0.620122	0.005858
72	relu	0.04	(85, 50)	lbfgs	0.617952	0.001734
73	tanh	0.04	(30, 20)	lbfgs	0.612343	0.002938
74	relu	0.75	(40,)	adam	0.611261	0.005259
75	tanh	0.18	(40,)	adam	0.61006	0.005921
76	relu	0.18	(100,)	lbfgs	0.609191	0.002677
77	tanh	0.04	(40,)	adam	0.607384	0.005943
78	tanh	0.01	(40,)	adam	0.607378	0.005943
79	tanh	0	(40,)	adam	0.607214	0.005945
80	relu	0.75	(25,)	adam	0.606949	0.005923
81	tanh	0.75	(30, 20)	adam	0.601959	0.006067

82	relu	0.18	(40,)	lbfgs	0.596912	0.003105
83	tanh	0.18	(75,)	adam	0.573018	0.006236
84	tanh	0	(75,)	adam	0.565009	0.006296
85	tanh	0.01	(75,)	adam	0.564981	0.006297
86	relu	3.16	(75,)	sgd	0.564173	0.006149
87	tanh	0.04	(75,)	adam	0.564161	0.006302
88	relu	3.16	(40,)	sgd	0.564065	0.006083
89	relu	3.16	(100,)	adam	0.561376	0.00634
90	relu	3.16	(50,)	adam	0.539099	0.006492
91	tanh	0.04	(30, 20)	adam	0.526722	0.006515
92	tanh	0.01	(30, 20)	adam	0.521697	0.00654
93	tanh	0	(30, 20)	adam	0.521464	0.006541
94	tanh	3.16	(25,)	sgd	0.517545	0.006693
95	relu	13.34	(40,)	lbfgs	0.511773	0.006694
96	relu	13.34	(50,)	lbfgs	0.508937	0.006708
97	relu	13.34	(75,)	lbfgs	0.508876	0.006718
98	relu	3.16	(40,)	adam	0.50875	0.006698
99	relu	0.18	(25,)	adam	0.506533	0.00651
100	tanh	0.75	(100,)	adam	0.500248	0.006795
101	tanh	0.75	(50, 40)	adam	0.496587	0.006809
102	relu	13.34	(100,)	lbfgs	0.493222	0.006793
103	tanh	0.75	(85, 50)	adam	0.492896	0.006853

104	relu	3.16	(25,)	sgd	0.492742	0.006782
105	tanh	0.75	(75,)	adam	0.488238	0.006854
106	relu	3.16	(25,)	adam	0.481587	0.006876
107	relu	13.34	(25,)	lbfgs	0.475898	0.006946
108	relu	0.04	(40,)	lbfgs	0.460652	0.003313
109	relu	0.18	(75,)	adam	0.458647	0.005954
110	relu	0.18	(75,)	lbfgs	0.456982	0.002729
111	tanh	13.34	(40,)	lbfgs	0.450873	0.007113
112	tanh	13.34	(25,)	lbfgs	0.449426	0.00712
113	tanh	13.34	(75,)	lbfgs	0.449314	0.00712
114	tanh	13.34	(50,)	lbfgs	0.448884	0.007123
115	tanh	13.34	(100,)	lbfgs	0.447098	0.007135
116	tanh	3.16	(40,)	sgd	0.443861	0.007134
117	relu	0.04	(25,)	adam	0.439521	0.006847
118	tanh	0.75	(50,)	adam	0.43662	0.007153
119	relu	0.01	(85, 50)	adam	0.433897	0.005827
120	relu	3.16	(75,)	adam	0.430308	0.007228
121	relu	0.01	(25,)	adam	0.427099	0.006928
122	relu	0.75	(50, 40)	sgd	0.425121	0.007059
123	relu	0	(25,)	adam	0.424051	0.006945
124	tanh	0.18	(25,)	adam	0.41786	0.007205
125	tanh	3.16	(75,)	sgd	0.383621	0.007519

126	relu	0.18	(25,)	lbfgs	0.382458	0.003403
127	tanh	0.04	(50, 40)	lbfgs	0.372588	0.002848
128	relu	0	(85, 50)	adam	0.3629	0.006141
129	tanh	0.04	(25,)	adam	0.34974	0.00762
130	tanh	0.01	(25,)	adam	0.344578	0.007659
131	tanh	0	(25,)	adam	0.344081	0.00766
132	relu	0.75	(25,)	sgd	0.343815	0.007815
133	relu	0.04	(30, 20)	adam	0.343011	0.00705
134	relu	13.34	(30, 20)	lbfgs	0.337146	0.007791
135	relu	0.18	(50, 40)	sgd	0.335965	0.007697
136	relu	13.34	(85, 50)	lbfgs	0.334695	0.007808
137	relu	0	(50, 40)	sgd	0.334592	0.007704
138	relu	0.01	(50, 40)	sgd	0.33446	0.007705
139	relu	0.04	(50, 40)	sgd	0.334395	0.007705
140	relu	13.34	(50, 40)	lbfgs	0.334367	0.007812
141	tanh	0.18	(50,)	adam	0.327277	0.00778
142	tanh	3.16	(25,)	adam	0.322707	0.007882
143	tanh	3.16	(100,)	sgd	0.320328	0.007897
144	relu	3.16	(30, 20)	sgd	0.317784	0.007896
145	tanh	0.75	(50,)	sgd	0.31584	0.00787
146	tanh	0.18	(50,)	sgd	0.315591	0.007873
147	tanh	0	(50,)	sgd	0.315585	0.007873

148	tanh	0.01	(50,)	sgd	0.31558	0.007873
149	tanh	0.04	(50,)	sgd	0.315494	0.007873
150	tanh	3.16	(50,)	sgd	0.309651	0.007932
151	tanh	0.75	(75,)	sgd	0.303631	0.007977
152	tanh	0.04	(50,)	adam	0.302499	0.007934
153	tanh	0.18	(100,)	adam	0.302347	0.007768
154	tanh	0	(50,)	adam	0.302257	0.007935
155	tanh	0.01	(50,)	adam	0.301954	0.007937
156	relu	0.18	(25,)	sgd	0.288008	0.00813
157	relu	0.04	(25,)	sgd	0.276263	0.008193
158	relu	0.01	(25,)	sgd	0.274182	0.008204
159	relu	0	(25,)	sgd	0.273486	0.008208
160	relu	0.75	(50,)	adam	0.273119	0.007127
161	tanh	3.16	(40,)	adam	0.268663	0.008178
162	relu	3.16	(85, 50)	sgd	0.268505	0.00818
163	relu	3.16	(30, 20)	adam	0.265886	0.008199
164	tanh	13.34	(85, 50)	lbfgs	0.263578	0.008211
165	tanh	3.16	(50,)	adam	0.259804	0.008231
166	tanh	13.34	(50, 40)	lbfgs	0.25876	0.008237
167	tanh	13.34	(30, 20)	lbfgs	0.254871	0.008257
168	tanh	0.75	(85, 50)	sgd	0.254262	0.008238
169	tanh	3.16	(75,)	adam	0.251842	0.008275

170	tanh	3.16	(100,)	adam	0.251394	0.008278
171	relu	3.16	(50, 40)	sgd	0.250133	0.008277
172	tanh	3.16	(30, 20)	sgd	0.23853	0.008347
173	tanh	0	(100,)	adam	0.233651	0.008157
174	tanh	0.01	(100,)	adam	0.232778	0.008162
175	tanh	0.04	(100,)	adam	0.231741	0.008164
176	relu	0.01	(30, 20)	adam	0.226132	0.007488
177	tanh	0.18	(100,)	sgd	0.226111	0.008433
178	tanh	0.04	(100,)	sgd	0.225968	0.008433
179	tanh	0.01	(100,)	sgd	0.22595	0.008433
180	tanh	0	(100,)	sgd	0.225943	0.008433
181	tanh	0.75	(100,)	sgd	0.225777	0.008433
182	relu	0	(30, 20)	adam	0.221203	0.007519
183	relu	3.16	(50, 40)	adam	0.219402	0.008445
184	tanh	0.75	(30, 20)	sgd	0.218665	0.008493
185	relu	0.04	(75,)	adam	0.215355	0.007102
186	tanh	0.18	(75,)	sgd	0.20944	0.008423
187	tanh	0.18	(50, 40)	lbfgs	0.201229	0.0357
188	tanh	0.04	(75,)	sgd	0.199966	0.08468
189	tanh	0.01	(75,)	sgd	0.195853	0.08481
190	tanh	0	(75,)	sgd	0.195385	0.08485
191	relu	3.16	(85, 50)	adam	0.188542	0.08611

192	relu	0.01	(75,)	adam	0.17154	0.07291
193	relu	0	(75,)	adam	0.164167	0.07301
194	tanh	3.16	(50, 40)	sgd	0.163526	0.0874
195	relu	0.18	(100,)	adam	0.153853	0.07662
196	tanh	3.16	(85, 50)	sgd	0.146264	0.0883
197	tanh	3.16	(30, 20)	adam	0.135537	0.08885
198	tanh	0.18	(30, 20)	sgd	0.123969	0.09025
199	tanh	3.16	(50, 40)	adam	0.120878	0.08958
200	tanh	3.16	(85, 50)	adam	0.11756	0.08974
201	tanh	0.04	(30, 20)	sgd	0.114146	0.09077
202	tanh	0.01	(30, 20)	sgd	0.111834	0.09088
203	tanh	0	(30, 20)	sgd	0.111139	0.09091
204	relu	13.34	(100,)	adam	0.091327	0.09106
205	relu	56.23	(50,)	lbfgs	0.082762	0.09148
206	relu	56.23	(40,)	lbfgs	0.082653	0.09147
207	relu	56.23	(100,)	lbfgs	0.082347	0.09149
208	relu	56.23	(75,)	lbfgs	0.082294	0.0915
209	relu	56.23	(25,)	lbfgs	0.081814	0.09152
210	relu	13.34	(50,)	adam	0.081606	0.09154
211	tanh	0.75	(50, 40)	sgd	0.076355	0.09039
212	tanh	0.18	(85, 50)	sgd	0.06747	0.0921
213	tanh	0.18	(100,)	lbfgs	0.0646	0.0366

214	tanh	56.23	(25,)	lbfgs	0.064173	0.09239
215	tanh	0.04	(85, 50)	sgd	0.063447	0.09231
216	tanh	56.23	(40,)	lbfgs	0.062761	0.09246
217	tanh	0.01	(85, 50)	sgd	0.062569	0.09234
218	tanh	0	(85, 50)	sgd	0.062485	0.09235
219	tanh	56.23	(50,)	lbfgs	0.060124	0.09259
220	tanh	56.23	(75,)	lbfgs	0.059801	0.0926
221	tanh	56.23	(100,)	lbfgs	0.055597	0.09281
222	tanh	13.34	(100,)	adam	0.055445	0.09282
223	relu	13.34	(40,)	adam	0.05003	0.09308
224	relu	13.34	(50,)	sgd	0.047503	0.09319
225	relu	13.34	(25,)	adam	0.042396	0.09343
226	tanh	13.34	(100,)	sgd	0.035687	0.09378
227	tanh	13.34	(40,)	sgd	0.03495	0.09382
228	relu	13.34	(100,)	sgd	0.029614	0.09405
229	tanh	13.34	(25,)	sgd	0.027032	0.09419
230	tanh	13.34	(50,)	sgd	0.02589	0.09424
231	relu	13.34	(75,)	sgd	0.021091	0.09445
232	tanh	13.34	(50,)	adam	0.02109	0.09448
233	tanh	13.34	(75,)	sgd	0.020606	0.09448
234	tanh	13.34	(25,)	adam	0.018789	0.09458
235	relu	13.34	(40,)	sgd	0.017215	0.09466

236	tanh	13.34	(40,)	adam	0.012341	0.09488
237	tanh	13.34	(75,)	adam	0.004827	0.09524
238	relu	13.34	(25,)	sgd	0.001846	0.09537
239	relu	13.34	(75,)	adam	-0.02161	0.09647
240	tanh	0.18	(50, 40)	sgd	-0.05744	0.09622
241	tanh	0.04	(50, 40)	sgd	-0.06622	0.0966
242	tanh	0.01	(50, 40)	sgd	-0.06804	0.09667
243	tanh	0	(50, 40)	sgd	-0.06864	0.09669
244	tanh	0.18	(50,)	lbfgs	-0.0717	0.03539
245	tanh	0.18	(75,)	lbfgs	-0.11618	0.03443
246	relu	56.23	(100,)	adam	-0.1665	0.010304
247	tanh	13.34	(30, 20)	sgd	-0.16874	0.010313
248	relu	56.23	(50,)	adam	-0.17356	0.010334
249	tanh	13.34	(50, 40)	sgd	-0.17396	0.010336
250	tanh	13.34	(85, 50)	sgd	-0.17454	0.010338
251	relu	13.34	(30, 20)	sgd	-0.17466	0.010339
252	relu	56.23	(25,)	sgd	-0.17487	0.01034
253	tanh	56.23	(25,)	sgd	-0.17512	0.010341
254	tanh	56.23	(75,)	sgd	-0.17647	0.010347
255	relu	13.34	(85, 50)	sgd	-0.17716	0.01035
256	tanh	56.23	(40,)	sgd	-0.17721	0.01035
257	relu	13.34	(50, 40)	sgd	-0.17802	0.010353

258	relu	56.23	(40,)	sgd	-0.17829	0.010355
259	relu	56.23	(75,)	sgd	-0.17835	0.010355
260	relu	237.14	(75,)	lbfgs	-0.1785	0.010355
261	relu	1000	(75,)	lbfgs	-0.1785	0.010355
262	tanh	1000	(100,)	lbfgs	-0.17851	0.010355
263	relu	237.14	(85, 50)	lbfgs	-0.17851	0.010355
264	tanh	1000	(85, 50)	lbfgs	-0.17852	0.010355
265	relu	1000	(50,)	lbfgs	-0.17852	0.010355
266	tanh	237.14	(40,)	lbfgs	-0.17853	0.010356
267	relu	56.23	(30, 20)	lbfgs	-0.17853	0.010356
268	tanh	1000	(75,)	lbfgs	-0.17853	0.010356
269	tanh	1000	(25,)	lbfgs	-0.17854	0.010356
270	tanh	56.23	(30, 20)	lbfgs	-0.17854	0.010356
271	relu	237.14	(50,)	lbfgs	-0.17855	0.010356
272	relu	56.23	(50, 40)	lbfgs	-0.17855	0.010356
273	tanh	56.23	(50, 40)	lbfgs	-0.17855	0.010356
274	relu	56.23	(85, 50)	lbfgs	-0.17855	0.010356
275	relu	237.14	(100,)	lbfgs	-0.17855	0.010356
276	tanh	1000	(30, 20)	lbfgs	-0.17856	0.010356
277	relu	1000	(25,)	lbfgs	-0.17856	0.010356
278	tanh	237.14	(50,)	lbfgs	-0.17856	0.010356
279	tanh	1000	(50, 40)	lbfgs	-0.17856	0.010356

280	relu	237.14	(25,)	lbfgs	-0.17857	0.010356
281	relu	1000	(30, 20)	lbfgs	-0.17857	0.010356
282	tanh	56.23	(85, 50)	lbfgs	-0.17857	0.010356
283	tanh	237.14	(100,)	lbfgs	-0.17857	0.010356
284	tanh	237.14	(85, 50)	lbfgs	-0.17857	0.010356
285	relu	1000	(85, 50)	lbfgs	-0.17857	0.010356
286	tanh	1000	(40,)	lbfgs	-0.17858	0.010356
287	tanh	237.14	(25,)	lbfgs	-0.17858	0.010356
288	relu	1000	(100,)	lbfgs	-0.17858	0.010356
289	relu	237.14	(50, 40)	lbfgs	-0.17858	0.010356
290	tanh	237.14	(75,)	lbfgs	-0.17859	0.010356
291	relu	1000	(50, 40)	lbfgs	-0.17859	0.010356
292	tanh	56.23	(100,)	sgd	-0.17859	0.010356
293	tanh	56.23	(100,)	adam	-0.1786	0.010357
294	tanh	237.14	(50, 40)	lbfgs	-0.1786	0.010356
295	tanh	237.14	(30, 20)	lbfgs	-0.1786	0.010356
296	relu	237.14	(40,)	lbfgs	-0.17861	0.010356
297	relu	237.14	(30, 20)	lbfgs	-0.17861	0.010356
298	relu	1000	(40,)	lbfgs	-0.17864	0.010356
299	tanh	1000	(50,)	lbfgs	-0.17864	0.010356
300	relu	56.23	(50,)	sgd	-0.17979	0.010361
301	relu	56.23	(30, 20)	sgd	-0.18025	0.010363

302	relu	56.23	(100,)	sgd	-0.18035	0.010364
303	tanh	56.23	(50,)	sgd	-0.18081	0.010366
304	relu	56.23	(85, 50)	sgd	-0.18093	0.010366
305	tanh	1000	(50, 40)	adam	-0.18122	0.010367
306	relu	56.23	(25,)	adam	-0.18137	0.010368
307	relu	1000	(75,)	adam	-0.1815	0.010368
308	relu	1000	(50, 40)	adam	-0.1819	0.01037
309	relu	0.04	(50,)	lbfgs	-0.18267	0.003068
310	tanh	1000	(85, 50)	adam	-0.183	0.010375
311	relu	56.23	(75,)	adam	-0.18305	0.010375
312	relu	13.34	(30, 20)	adam	-0.18444	0.010381
313	relu	56.23	(50, 40)	sgd	-0.18449	0.010382
314	tanh	237.14	(50, 40)	adam	-0.18485	0.010383
315	tanh	56.23	(25,)	adam	-0.18537	0.010386
316	relu	13.34	(50, 40)	adam	-0.18539	0.010385
317	tanh	56.23	(85, 50)	sgd	-0.18542	0.010386
318	tanh	1000	(25,)	adam	-0.18561	0.010386
319	tanh	13.34	(50, 40)	adam	-0.18571	0.010387
320	tanh	56.23	(75,)	adam	-0.18586	0.010387
321	tanh	56.23	(50,)	adam	-0.18615	0.010389
322	tanh	13.34	(85, 50)	adam	-0.18661	0.010391
323	relu	237.14	(50, 40)	adam	-0.18666	0.010391

324	relu	56.23	(40,)	adam	-0.18719	0.010394
325	tanh	56.23	(50, 40)	sgd	-0.1873	0.010394
326	tanh	237.14	(85, 50)	adam	-0.18756	0.010395
327	relu	237.14	(75,)	adam	-0.18767	0.010395
328	tanh	56.23	(50, 40)	adam	-0.1885	0.010399
329	tanh	56.23	(40,)	adam	-0.18855	0.0104
330	relu	13.34	(85, 50)	adam	-0.18858	0.0104
331	tanh	13.34	(30, 20)	adam	-0.18862	0.0104
332	relu	1000	(85, 50)	adam	-0.18867	0.0104
333	relu	56.23	(50, 40)	adam	-0.18874	0.0104
334	relu	237.14	(85, 50)	sgd	-0.18883	0.0104
335	tanh	56.23	(30, 20)	sgd	-0.19047	0.010408
336	tanh	56.23	(85, 50)	adam	-0.19072	0.010409
337	tanh	1000	(75,)	adam	-0.19081	0.010409
338	relu	237.14	(25,)	sgd	-0.19143	0.010412
339	relu	237.14	(30, 20)	sgd	-0.19147	0.010412
340	relu	1000	(25,)	adam	-0.1915	0.010412
341	tanh	237.14	(25,)	adam	-0.19166	0.010413
342	tanh	1000	(30, 20)	adam	-0.19356	0.010421
343	relu	56.23	(85, 50)	adam	-0.19512	0.010428
344	relu	237.14	(50, 40)	sgd	-0.19538	0.010429
345	relu	237.14	(25,)	adam	-0.19621	0.010433

346	tanh	1000	(40,)	adam	-0.19637	0.010433
347	relu	237.14	(85, 50)	adam	-0.19644	0.010434
348	tanh	237.14	(25,)	sgd	-0.19699	0.010436
349	tanh	237.14	(85, 50)	sgd	-0.19701	0.010436
350	tanh	237.14	(75,)	adam	-0.1985	0.010443
351	relu	1000	(30, 20)	sgd	-0.19926	0.010446
352	relu	237.14	(40,)	sgd	-0.19958	0.010447
353	relu	1000	(85, 50)	sgd	-0.1996	0.010447
354	tanh	237.14	(50, 40)	sgd	-0.19972	0.010448
355	tanh	1000	(30, 20)	sgd	-0.20072	0.010452
356	relu	1000	(40,)	sgd	-0.20078	0.010452
357	tanh	1000	(85, 50)	sgd	-0.20083	0.010453
358	relu	1000	(50, 40)	sgd	-0.20085	0.010453
359	relu	1000	(25,)	sgd	-0.20091	0.010453
360	relu	1000	(100,)	sgd	-0.2014	0.010455
361	relu	1000	(50,)	sgd	-0.20143	0.010455
362	tanh	1000	(50, 40)	sgd	-0.2017	0.010456
363	relu	1000	(75,)	sgd	-0.20206	0.010458
364	relu	237.14	(75,)	sgd	-0.20259	0.01046
365	tanh	237.14	(30, 20)	sgd	-0.20281	0.010461
366	tanh	1000	(40,)	sgd	-0.20287	0.010461
367	tanh	1000	(25,)	sgd	-0.20293	0.010462

368	tanh	1000	(50,)	sgd	-0.20308	0.010462
369	tanh	237.14	(75,)	sgd	-0.20341	0.010464
370	tanh	237.14	(30, 20)	adam	-0.20348	0.010464
371	tanh	1000	(75,)	sgd	-0.20364	0.010465
372	tanh	56.23	(30, 20)	adam	-0.20384	0.010466
373	tanh	237.14	(40,)	adam	-0.20389	0.010466
374	tanh	1000	(100,)	sgd	-0.2041	0.010467
375	relu	56.23	(30, 20)	adam	-0.2044	0.010468
376	relu	1000	(30, 20)	adam	-0.20559	0.010473
377	relu	1000	(40,)	adam	-0.20609	0.010475
378	tanh	237.14	(40,)	sgd	-0.2061	0.010475
379	relu	237.14	(50,)	sgd	-0.20621	0.010476
380	relu	237.14	(100,)	sgd	-0.20628	0.010476
381	tanh	237.14	(50,)	sgd	-0.20932	0.010489
382	tanh	237.14	(100,)	sgd	-0.21045	0.010494
383	relu	237.14	(40,)	adam	-0.21107	0.010497
384	relu	237.14	(30, 20)	adam	-0.2132	0.010506
385	tanh	237.14	(50,)	adam	-0.21503	0.010514
386	tanh	237.14	(100,)	adam	-0.21669	0.010521
387	tanh	1000	(50,)	adam	-0.21889	0.010531
388	relu	237.14	(100,)	adam	-0.21971	0.010535
389	relu	237.14	(50,)	adam	-0.22514	0.010557

390	tanh	1000	(100,)	adam	-0.22634	0.010562
391	relu	1000	(100,)	adam	-0.22886	0.010573
392	relu	1000	(50,)	adam	-0.2321	0.010587
393	relu	0.04	(100,)	adam	-0.31324	0.09426
394	tanh	0.04	(40,)	lbfgs	-0.39518	0.03722
395	relu	0.01	(100,)	adam	-0.41457	0.09755
396	relu	0	(100,)	adam	-0.44941	0.09874
397	relu	0	(50,)	adam	-0.5108	0.01006
398	relu	0.01	(50,)	adam	-0.51846	0.010093
399	relu	0.04	(50,)	adam	-0.55986	0.010173
400	relu	0.75	(30, 20)	sgd	-0.64061	0.011693
401	relu	0.18	(50,)	adam	-0.66627	0.010396
402	relu	0.04	(25,)	lbfgs	-0.69005	0.03687
403	tanh	0.04	(50,)	lbfgs	-0.86187	0.03705
404	relu	0.18	(30, 20)	sgd	-1.12846	0.013236
405	relu	0.04	(30, 20)	sgd	-1.26957	0.013619
406	relu	0.01	(30, 20)	sgd	-1.30094	0.013706
407	relu	0	(30, 20)	sgd	-1.3111	0.013736
408	relu	0.75	(100,)	sgd	-1.52959	0.015612
409	relu	0.04	(75,)	lbfgs	-1.76873	0.02458
410	tanh	0.01	(50, 40)	lbfgs	-1.93257	0.02614
411	tanh	0.01	(40,)	lbfgs	-2.4585	0.03593

412	relu	0.18	(100,)	sgd	-2.66718	0.018914
413	relu	0.04	(100,)	sgd	-2.86835	0.019481
414	relu	0.01	(100,)	sgd	-2.9057	0.019577
415	relu	0	(100,)	sgd	-2.92147	0.019609
416	relu	0.01	(30, 20)	lbfgs	-2.94657	0.02398
417	relu	0.01	(25,)	lbfgs	-4.19782	0.0378
418	relu	0.75	(50,)	sgd	-4.92352	0.020921
419	relu	0.18	(50, 40)	lbfgs	-5.57389	0.02481
420	tanh	0.04	(75,)	lbfgs	-5.71469	0.04255
421	tanh	0.04	(25,)	lbfgs	-6.03368	0.03567
422	tanh	0.75	(25,)	sgd	-6.21596	0.02543
423	relu	0.75	(85, 50)	sgd	-7.63181	0.023757
424	relu	0.18	(50,)	sgd	-7.98646	0.025518
425	relu	0.01	(50,)	lbfgs	-8.46708	0.003322
426	relu	0.01	(75,)	lbfgs	-8.55124	0.002479
427	relu	0.04	(50,)	sgd	-8.58005	0.026287
428	relu	0.01	(50,)	sgd	-8.64919	0.02639
429	relu	0	(50,)	sgd	-8.67438	0.02643
430	tanh	0.18	(25,)	sgd	-9.47404	0.030385
431	relu	0.18	(85, 50)	sgd	-10.1067	0.028966
432	tanh	0.04	(25,)	sgd	-10.162	0.031234
433	tanh	0.01	(25,)	sgd	-10.2445	0.031398

434	tanh	0	(25,)	sgd	-10.2721	0.031437
435	relu	0.04	(85, 50)	sgd	-10.485	0.029519
436	relu	0.01	(85, 50)	sgd	-10.6313	0.029696
437	relu	0	(85, 50)	sgd	-10.6823	0.029759
438	relu	0.01	(100,)	lbfgs	-10.8414	0.02296
439	relu	0.75	(75,)	sgd	-11.3916	0.029297
440	relu	0.18	(75,)	sgd	-17.2194	0.035231
441	relu	0.04	(75,)	sgd	-18.4286	0.03625
442	relu	0.18	(40,)	adam	-18.4406	0.029025
443	relu	0.01	(75,)	sgd	-18.7199	0.036458
444	relu	0	(75,)	sgd	-18.7742	0.036506
445	tanh	0.01	(50,)	lbfgs	-20.1703	0.03453
446	relu	0.04	(40,)	adam	-27.5573	0.034847
447	relu	0.01	(40,)	adam	-28.3249	0.035479
448	relu	0	(40,)	adam	-28.7575	0.035606
449	relu	0	(25,)	lbfgs	-29.4514	0.04118
450	relu	0.01	(40,)	lbfgs	-43.6213	0.03581
451	tanh	0.04	(100,)	lbfgs	-76.3588	0.03641
452	relu	0	(40,)	lbfgs	-99.6183	0.0385
453	tanh	0.01	(75,)	lbfgs	-121.574	0.03725
454	tanh	0.01	(30, 20)	lbfgs	-127.41	0.02749
455	relu	0	(30, 20)	lbfgs	-131.451	0.02474

456	tanh	0.01	(25,)	lbfgs	-200.114	0.03679
457	tanh	0	(50, 40)	lbfgs	-210.169	0.025
458	tanh	0	(50,)	lbfgs	-236.55	0.03136
459	relu	0.75	(40,)	sgd	-972.959	0.237179
460	relu	0	(75,)	lbfgs	-1049.7	0.02584
461	tanh	0.01	(85, 50)	lbfgs	-1128.37	0.02737
462	tanh	0.04	(85, 50)	lbfgs	-1211.66	0.02996
463	tanh	0	(100,)	lbfgs	-1310.13	0.03076
464	relu	0.18	(40,)	sgd	-1752.31	0.314211
465	relu	0.04	(40,)	sgd	-1887.71	0.326896
466	relu	0.01	(40,)	sgd	-1930.66	0.329733
467	relu	0	(40,)	sgd	-1938.61	0.330371
468	tanh	0.01	(100,)	lbfgs	-4141.78	0.03343
469	relu	0.01	(85, 50)	lbfgs	-6399.93	0.01374
470	tanh	0	(40,)	lbfgs	-6653.09	0.03273
471	relu	0.04	(50, 40)	lbfgs	-9200.06	0.01923
472	relu	0.01	(50, 40)	lbfgs	-18230	0.01613
473	relu	0	(100,)	lbfgs	-30227.1	0.02286
474	relu	0	(50,)	lbfgs	-54244.4	0.03465
475	tanh	0	(85, 50)	lbfgs	-58388.7	0.0259
476	tanh	0	(25,)	lbfgs	-227222	0.03427
477	tanh	0	(30, 20)	lbfgs	-1638014	0.02615

478	relu	0	(85, 50)	lbfgs	-4561176	0.01367
479	tanh	0	(75,)	lbfgs	-1.6E+09	0.03294
480	relu	0	(50, 40)	lbfgs	-7.3E+10	0.01595